DOKUZ EYLÜL UNIVERSITY
GRADUATE SCHOOL OF NATURAL AND APPLIED SCIENCES

OUT – OF – PLANE DYNAMIC STABILITY ANALYSIS OF CURVED BEAMS UNDER DISTRIBUTED DYNAMIC LOADING

by
Şeref ÇİMEN

March, 2008
İZMİR

OUT – OF – PLANE DYNAMIC STABILITY ANALYSIS OF CURVED BEAMS UNDER DISTRIBUTED DYNAMIC LOADING

A Thesis Submitted to the
Graduate School of Natural and Applied Sciences of Dokuz Eylul University
In Partial Fulfillment of the Requirements for the Degree of Master of Science in
Mechanical Engineering, Machine Theory and Dynamics Program

by
Şeref ÇİMEN

January, 2008
İZMİR

M.Sc THESIS EXAMINATION RESULT FORM

We have read the thesis entitled "**OUT – OF – PLANE DYNAMİC STABILITY ANALYSIS OF CURVED BEAMS UNDER DİSTRIBUTED DYNAMIC LOADING**" completed by **ŞEREF ÇİMEN** under supervision of **PROF. DR. MUSTAFA SABUNCU** and we certify that in our opinion it is fully adequate, in scope and in quality, as a thesis for the degree of Master of Science.

PROF. DR. MUSTAFA SABUNCU

Supervisor

PROF. DR. HİKMET H. ÇATAL

(Jury member)

YRD.DOÇ.DR.AYSUN BALTACI

(Jury member)

Prof.Dr. Cahit HELVACI
Director
Graduate School of Natural and Applied Sciences

ACKNOWLEDGEMENTS

I would like to thank to my supervisor Prof.Dr. Mustafa SABUNCU, for his help, guidance, criticism and encouragement thought the course of this work.

I would also like to thank to Research Assistant Dr. Hasan ÖZTÜRK, for his help, with valuable suggestions and discussions that they have provided me during the research.

I am also thankful to all my friends for their valuable help throughout this study.

I am especially very grateful to my family for their patience and support.

Şeref ÇİMEN

OUT – OF – PLANE DYNAMIC STABILITY ANALYSIS OF CURVED BEAMS UNDER DISTRIBUTED DYNAMIC LOADING

ABSTRACT

In this study, out of plane stability analysis of tapered cross-sectioned thin curved beams under uniformly distributed dynamic loads is investigated by using the Finite Element Method. Applying Lagrange's principles to the energy expressions, the equation of dynamic equilibrium of the system is obtained and the problem is reduced to an eigenvalue problem. Solutions referred to as Bolotin's approach are investigated for the dynamic stability analysis and the first unstable regions are examined. Out of plane vibration and out-plane buckling analyses are also studied. In addition, the results obtained from this study are compared with the results of other investigators in existing literature for the fundamental natural frequency and critical buckling load. The effects of subtended angle, variations of cross-section and, static and dynamic load parameters on the stability regions are shown in graphics. Moreover the results obtained with and without internal node for the vibration, buckling and dynamic stability are also compared.

Keywords : Dynamic stability, buckling, curved beam, finite element, internal node

EĞRİ ÇUBUKLARIN YAYILI DİNAMİK YÜK ALTINDA DÜZLEM DIŞI KARALILIK ANALİZİ

ÖZ

Bu çalışmada, sonlu elemanlar metodu kullanılarak lineer olmayan kesit değişimine sahip eğri çubukların, yayılı dinamik yük altındaki düzlem dışı kararlılığı sonlu elemanlar yöntemi kullanılarak araştırılmıştır. Dinamik kararlılık çözümleri için Bolotin [1], yaklaşımı kullanılmış ve Lagrange'in enerji denklemleri kullanılarak birinci kararsızlık bölgeleri incelenmiştir. Bunun yanında, düzlem dışı titreşim ve burkulma analizi yapılmıştır. Bu çalışmada, birinci doğal frekans ve burkulma yükü değerleri literatürde mevcut diğer araştırmacılar tarafından verilen sonuçlarla karşılaştırılmış ve eğri çubuğun merkez açısının, kesit değişimin ve, statik ve dinamik yük parametresinin kararlılık bölgeleri üzerindeki etkileri grafikler ile gösterilmiştir. Ayrıca ara nodlu ve ara nodsuz sonlu eleman kullanarak modellenen eğri çubuk için doğal frekans kritik burkulma yükü ve dinamik kararlılık analizleri karşılaştırılmıştır.

Anahtar Sözcükler: Dinamik kararlılık, burkulma, eğri çubuk, sonlu elemanlar metodu.

CONTENTS

Page

CHAPTER ONE
INTRODUCTION

The using of curved beams in high technology applications especially in turbine blades, bridges and outer space industry, has made elastic instability a problem of great importance. The problems which are examined in this branch of elasticity are related to those in the theory of vibrations and the stability of elastic systems. As in many other areas of learning that lie on the borderline of two fields, the theory of dynamic stability is now going through a period of intensive development.

The problem of determining the natural frequencies and mode shapes of vibration of curved beams under distributed dynamic loading is of importance in the design of turbine, bridge and outer space industry propellers.

The theory of dynamic stability has already opened the way for direct engineering applications. Parametrically excited vibrations are similar in appearance to the accompanying forced vibrations and can therefore qualify as ordinary resonance vibrations, by practical engineering standards. In a number of cases, however as in the presence of periodic vibrations the usual methods of damping on vibration isolation may break down and even bring about the opposite results. Although the vibrations may not threaten the structure or its normal operation, they can cause fatigue failure if they continue to act. Therefore, the study of the formation of parametric vibrations and the methods for the prevention of their occurrence is necessary in the various areas of mechanics, transportation and industrial construction.

Stability analysis of multiple degrees of freedom in parametric dynamic systems with periodic coefficients is a subject of recent interest, since the problem arises naturally in many physical situations; for example the dynamic stability of structures, under periodically varying loads, the stability of mechanisms with periodically varying inertia and stiffness coefficients and the stability of the steady state response of nonlinear systems.

Many investigations about in-plane and out-of-plane vibrations of curved beams have also been carried out.

Sabuncu (1978), investigated the vibration analysis of thin curved beams. He used several types of shape functions to develop different curved beam finite elements and pointed out the effect of displacement functions on the natural frequencies by comparing the results.

Sabir and Ashwel (1971), discussed the natural frequency analysis of circular aches deformed in plane. The finite elements developed by using different types of shape functions were employed in their analysis.

Petyt and Fleischer (1971), analyzed free vibrations of a curved beam for various boundary conditions.

Yıldırım (1996), performed the in-plane and out-plane free vibration analysis with the program developed using the transfer matrix method of a double-side symmetric and elastic curved beam.

Lee and Chao (2000), examined out-plane vibration of curved beams with a non-uniform cross-section for constant angle.

Kang, Bert and Striz (1995),discussed computation of the eigenvalues of the equations of motion governing the free in plane vibration including extensibility of the arch axis and the coupled out-of-plane twist-bending vibrations of circular arches using Differential Quadrature methods (DQM).

Rao and Gupta (2001) have studied the dynamic stiffness matrices for the out-of-plane vibration of curved beams using the Lagrange's equations and the dynamic equilibrium equations, respectively, and then solved for the natural frequencies.

Kawakami, Sakiyama and Matsuda (1995), derived the characteristic equation by applying the discrete Green functions and using the numerical integration to obtain the eigenvalues for both the in-plane and out-of-plane free vibrations of the non-uniform curved beams, where the formulation is much complicated than that of the classical approaches.

Cortinez, Piovan and Rossi (2000), developed out of plane vibration of continuous horizontally curved thin-walled beams with both open and close cross-sections.

Liu & Wu (2001), investigated in-plane free vibrations of circular arches using the generalized differential quadrature rule. The Kirchhoff assumptions for the these beams were considered and the neutral axis was taken as inextensible. They presented several examples of arches with uniform, continuously varying and stepped cross sections.

Ojalvo & Newman (1964), presented the frequencies of a cantilever ring segments.

Wu & Chiang (2003), investigated the natural frequencies and mode shapes for the radial bending vibrations of uniform circular arches by means of curved beam elements. The standard techniques were used to determine the natural frequencies and mode shapes for the curved beam with various boundary conditions and subtended angles.

Yoo, Kang and Davidson (1996), performed buckling analysis of curved beams with the finite element method.

Timoshenko and Gere (1961), studied the buckling analysis of hinged-hinged Bernoulli-Euler curved beams by using the analytical method.

Bazant and Cedolin (1991), discussed the buckling analysis of curved beams by using analytical and energy methods.

There have been many studies about the static and dynamic stability of mechanical systems such as curved beam.

Bolotin (1964), studied the dynamic stability problems of various kinds of structural components.

Abbas & Thomas (1978), developed a finite element model for the stability analysis of a Timoshenko beam resting on an elastic foundation and subjected to a periodic axial loads. The effect of an elastic foundation on the natural frequencies and static buckling loads of hinged-hinged and fixed free Timoshenko beams was investigated.

Öztürk, Yeşilyurt and Sabuncu (2006), investigated in-plane stability analysis of non-uniform cross-sectioned thin curved beams under uniformly distributed dynamic loads by using the Finite Element Method. In this study, two different finite element models, representing variations of cross-section, were developed by using simple strain functions in the analysis.

Banan, Karami and Farshad (1990), discussed Finite Elements analysis for the stability analysis of curved beams on elastic foundation.

Nair, Garg and Lai (1985), examined stability of a curved rail under a constant moving load using a linear theory, critical speeds of the moving load and the dynamic rail deflections and rotation.

Briseghella, Majarona & Pellegrino (1998), used the finite element method to find the regions of dynamic stability of beams and frames. A suitable numerical procedure was applied to obtain these regions and vibration frequency of the structures.

Yokoyama (1988), studied the parametric instability behavior of a Timoshenko beam resting on an elastic foundation of the Winkler type by the finite element technique.

Chen and Chern (1993), presented coupled bending-bending-torsion vibrations of a pretwisted rotating cantilever beams of fibre-reinforced material including shear deformation and rotary inertia. The free vibration and dynamic stability problems were discussed.

Papangelis & Trahair (1987), developed a flexural-torsional buckling theory for circular arches of doubly symmetric cross section. Non linear expressions for the axial and shear strains were derived, and these were substituted into the second variation of the total potential to obtain the buckling equation.

Yang & Kuo (1987), derived the nonlinear differential equations of equilibrium for a horizontally curved I-beam. Based on the principal of virtual displacements, the equilibrium of a bar was established for its deformed or buckled configuration using a Lagrangian approach.

Şakar, Öztürk & Sabuncu (2001), investigated the effects of variations of subtended angle and curvature of an arch, having in-plane curvature, on the natural frequencies, static and dynamic instability.

Yoo & Pfeiffer (1983), presented a general solution method of a system having coupled differential equations governing the elastic buckling of thin walled curved members. The finite element displacement method was formulated based on a variational principle.

There are many investigations about out of plane stability analysis of curved beams having symmetric and unsymmetric cross section. In this thesis the out of plane stability analysis of tapered cross-sectioned thin curved beams under uniformly distributed dynamic loads is investigated by using the Finite Element Method. Solutions referred to as Bolotin's approach are investigated for the dynamic stability analysis and the first unstable regions are examined. Since natural frequency and buckling load effect the determination of stability regions, the out of plane vibration and out-plane buckling analyses are also studied. Two finite element models, which are with and without internal node, are used for vibration and buckling analyses. In addition, the results obtained from this study are compared with the results of other investigators in existing literature for the fundamental natural frequency and critical buckling load. The effects of subtended angle, variations of cross-section and dynamic load parameter on the stability regions are shown in graphics.

Chapter 2 deals with the theories used to analyze the dynamic stability of elastic systems.

Chapter 3 deals with the theories used to analyze the finite element method

Chapter 4 contains the finite element model of a curved beam with and without internal node. The beam is assumed to have a rectangular cross section. It is also assumed that curved beams are having with small width/thickness ratio. As a result thin beam theory is applied by neglecting shear deformation and rotary inertia effects. The geometric stiffness, elastic stiffness and mass matrices of curved beams, representing stability and vibrations out-of-plane direction, are obtained by using the energy equations.

Chapter 5 covers the effects of the opening angle and curved beam dimensions on the vibration and, static (buckling analysis) and dynamic stability. All results are presented in tabular and/or graphical forms. The obtained results are discussed

Finally in chapter 6, conclusions drawn from the study are presented.

CHAPTER TWO
THEORY OF STABILITY ANALYSIS

2.1 Static stability

The modern use of steel and high-strength alloys in engineering structures, especially in bridges, ships and aircraft, has made elastic instability a problem of great importance. Urgent practical requirements have given rise in recent years to extensive theoretical investigations of the conditions governing the stability of beams, plates and shells.

The first problems of elastic instability, concerning lateral buckling of compressed members, were solved about 200 years ago by L. Euler. At that time the relatively low strength of materials necessitated stout structural members for which the question of elastic stability is not of primary importance. Thus Euler's theoretical solution, developed for slender bars, remained for a long time without a practical application. Only with the beginning of extensive steel constructions did the question of buckling of compression members become of practical importance. The use of steel led naturally to types of structures embodying slender compression members, thin plates and thin shells.

Stability problems can be treated in a general manner using the energy methods. As an introduction to such methods, the basic criteria for determining the stability of equilibrium is derived in this study for, conservative linearly elastic systems.

To establish the stability criteria, a function Π, called the potential of the system must be formulated. This function is expressed as the sum of the internal potential energy U (strain energy) and the potential energy Λ of the external forces that act on a system, i.e.,

$$\Pi = U + \Lambda \tag{2.1}$$

Disregarding a possible additive constant, $\Lambda = -W_e$, i.e., the loss of potential energy during the application of forces is equal to the work done on the system by external forces. Hence, equation (2.1) can be rewritten as

$$\Pi = U - W_e \tag{2.2}$$

As is known from classical mechanics, for equilibrium the total potential Π must be stationary, therefore its variation $\delta\Pi$ must equal zero,

$$\delta\Pi = \delta U - \delta W_e = 0 \tag{2.3}$$

For conservative, elastic systems this relation agrees with $\delta W_e = \delta W_{ei}$ equation (δW_{ei} : the external work on the internal elements of a body, δW_e : the total work), which states the virtual work principle. This condition can be used to determine the position of equilibrium. However, equation (2.3) cannot discern the type of equilibrium and there by establish the condition for the stability of equilibrium. Only by examining the higher order terms in the expression for increment in Π as given by Taylor's expansion must be examined. Such an expression is

$$\Delta\Pi = \delta\Pi + \frac{1}{2!}\delta^2\Pi + \frac{1}{3!}\delta^3\Pi + ... \tag{2.4}$$

Since for any type of equilibrium $\delta\Pi = 0$, it is the first nonvanishing term of this expansion that determines the types of equilibrium. For linear elastic systems the second term suffices. Thus, from equation (2.4), the stability criteria are

$\delta^2\Pi > 0$ for stable equilibrium

$\delta^2\Pi < 0$ for unstable equilibrium

$\delta^2\Pi = 0$ for neutral equilibrium associated with the critical load

The meaning of these expressions may be clarified by examining the simple example shown in figure 2.1, where the shaded surfaces represent three different types of Π functions. It can be concluded at once that the ball on the concave spherical surface (a) is in stable equilibrium, while the ball on the convex spherical surface (b) is in unstable equilibrium. The ball on the horizontal plane (c) is said to be in different or neutral equilibrium. The type of equilibrium can be ascertained by considering the energy of the system. In the first case (figure 2.1(a)) any displacement of the ball from its position of equilibrium will raise the center of gravity. A certain amount of work is required to produce such a displacement; thus the potential energy of the system increases for any small displacement from the position of equilibrium. In the second case (figure 2.1 (b)), any displacement from the position of equilibrium will decrease the potential energy of the system. Thus in the case of stable equilibrium the energy of the system is a minimum and in the case of unstable equilibrium it is a maximum. If the equilibrium is indifferent (figure 2.1 (c)), there is no change in energy during a displacement.

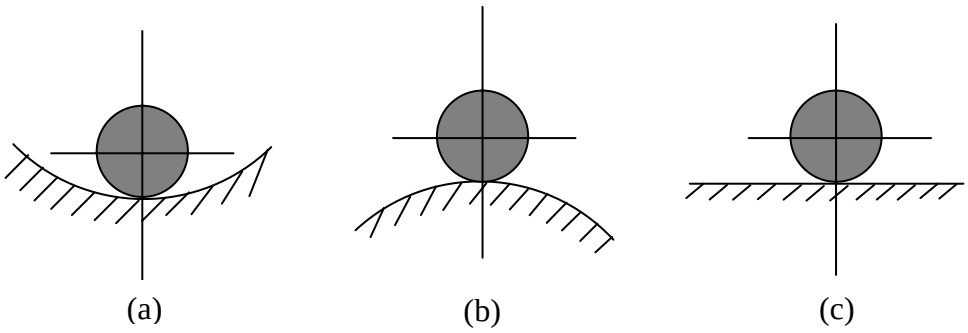

Figure 2.1 Three cases of equilibrium

For each of the systems shown in figure 2.1 stability depends only on the shape of the supporting surface and does not depend on the weight of the ball. In the case of a compressed column or plate it is found that the column or plate may be stable or unstable, depending on the magnitude of the axial load.

2.1.1 The formulation of static stability

If the displacements are large, then the deformed geometry will obviously differ significantly from the undeformed geometry. This results in a nonlinear strain-displacement relationship. Large displacement problems of this type are said to be "geometrically nonlinear" which is a feature of elastic instability problems. From the design point of view calculation of the critical loads of structures is of considerable importance. In general case the strain energy of a system,

$$U = \frac{1}{2}\{q\}^T [K_e]\{q\} \tag{2.5}$$

The additional strain energy which is function of applied external load

$$U_g = \frac{1}{2}\{q\}^T [K_g]\{q\} \tag{2.6}$$

In which $[K_e]$ and $[K_g]$ are elastic stiffness and geometric stiffness matrices.

The total potential energy of a system in equilibrium is constant when small displacements are given to the system. So

$$\delta(U + U_g) = 0 \tag{2.7}$$

$(U + U_g)$ and δ define the total potential energy and the change of the virtual displacements. Applying the above formulation to equations (2.5) and (2.6)

$$\left[[K_e] - P[K_g]\right]\{q\} = 0 \tag{2.8}$$

The roots of the eigenvalue equation (2.8) gives the buckling loads and the eigenvectors of this equation are the buckling mode shapes.

2.2 Dynamic stability

If the loading is nonconservative the loss of stability may not show up by the system going into another equilibrium state but by going into unbounded motion. To encompass this possibility we must consider the dynamic behavior of the system because stability is essentially a dynamic concept.

Whenever static loading of a particular kind causes a loss of static stability, vibrational loading of the same kind will cause a loss of dynamic stability. Such a loading is characterized by the fact that it is contained as a parameter on the left hand side of the equations of perturbed equilibrium (or motion). We will call such loading parametric; this term is more appropriate because it indicates the relation to the phenomenon of parametric resonance.

In the mechanical systems, parametric excitation occurs due to the following reasons;

a) periodic change in rigidity
b) periodic change in inertia
c) periodic change in the loading of the system.

In this section firstly the differential equation related with dynamic stability is introduced and then, the determination of boundaries of the regions of instability and the amplitudes of parametrically excited vibrations for multi-degrees of freedom systems is presented.

An important special case of linear variational equations with variable coefficients occurs when the coefficient functions are periodic. Owing to their great practical importance in the theory of vibrations, a special theory has even been developed for the systems of differential equations with periodic coefficients are known as Mathieu-Hill differential equation. The Hill differential equation is in the following form,

$$\ddot{y} + [a - b f(t)] y = 0 \qquad (2.9)$$

in which a and b are constant parameters, and f(t) is a function having the period T. The prime denotes differentiation with respect to time. If $f(t) = 2\cos 2t$ substituted into the Hill differential equation, the Mathieu differential equation which may be described a system that is subjected to parametric excitation is obtained in the standard form as

$$\ddot{y} + [a - 2b\cos 2t] y = 0 \qquad (2.10)$$

The results of solving Mathieu's equation (2.10) for two different combinations of a and b are shown in figure 2.2. Although the parameter b of the system is the same in both cases (b=0,1), the vibrations are greatly different because of the difference between the values of the parameter a (a=1; a=1,2). In the first case, they increase, i.e., the system is dynamically unstable, while in the second case they remain bounded, i.e., the system is dynamically stable.

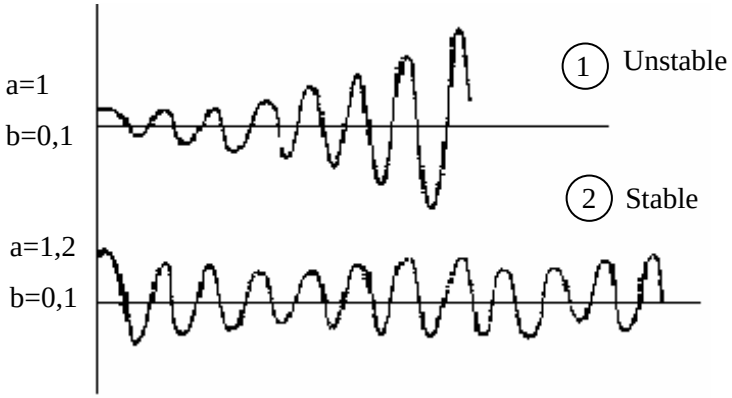

Figure 2.2 Two solutions of Mathieu's equation

The greatest importance, for practical purpose, is attached to the boundaries between the regions of stable and unstable solutions. This problem has been well studied, and the final results have been presented in the form of a diagram plotted in the plane of the parameters a and b. It is called the Haines-Strett diagram. Figure 2.3 shows part of a Haines-Strett diagram for small values of the parameter b. Any given system having the parameters a and b corresponds to the point with the co-ordinates

a and b on the Haines-Strett diagram. If the representative point is in the shaded parts of the diagram, the system is dynamically unstable, while stable systems correspond to representative points in the unshaded parts. The shaded regions are called the regions of dynamic instability.

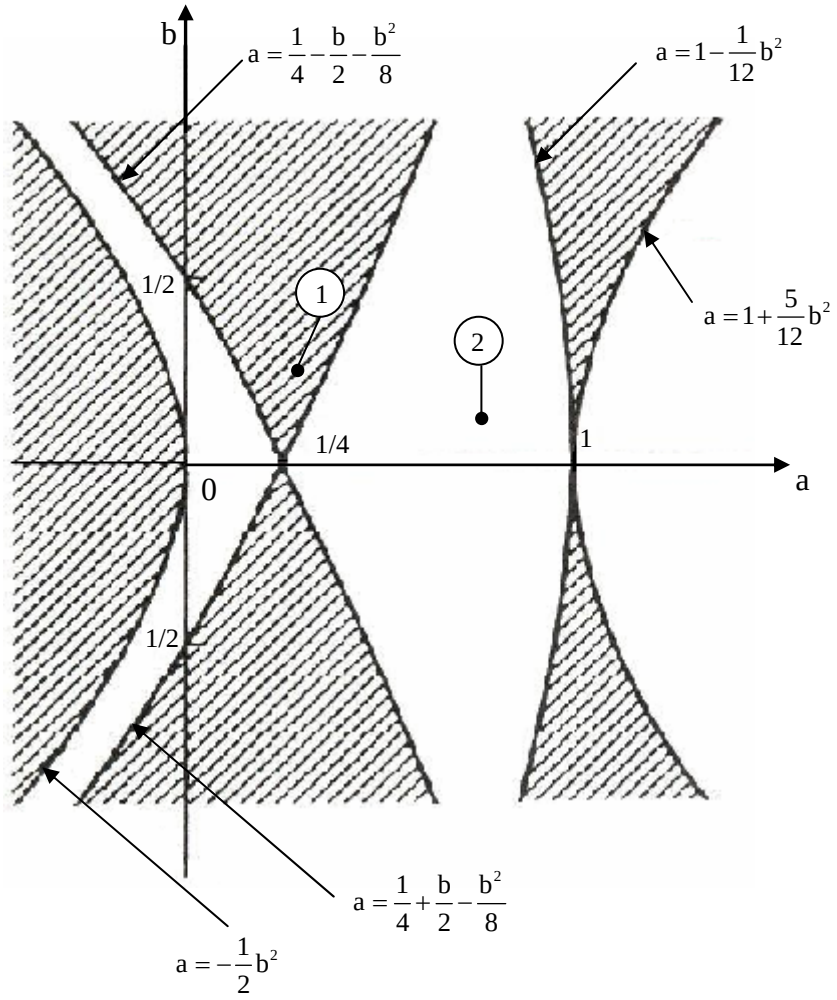

Figure 2.3 Part of Haines-Strett diagram the points ① and ② correspond to the solutions 1 and 2 in figure 2.2

As an example, the diagram in figure 2.3 shows the points 1 and 2 corresponding to the parameter a_1=1 and b_1=0,1, and a_2=1,2 and b_2=0,1. The point 1 is in the region of dynamic instability and the vibration occurs with increasing amplitude as shown in figure 2.2. The point 2 is in the stable region and it corresponds to motion with a limited amplitude.

2.2.1 The formulation of dynamic stability

The matrix equation for the free vibration of an axially loaded system can be written as:

$$[M]\{\ddot{q}\}+[K_e]\{q\}-[K_g]\{q\}=0 \tag{2.11}$$

where

$\{q\}$ is the generalized coordinates

$[M]$ is the inertia matrix

$[K_e]$ is the elastic stiffness matrix

$[K_g]$ is the geometric stiffness matrix, which is a function of the compressive axial load P(t).

For a system subjected to a periodic force

$$P(t)=P_o+P_t f(t) \tag{2.12}$$

The static and time dependent components of the load can be represented as a fraction of the fundamental static buckling load P*, in which $P_o=\alpha P^*$, $P_t=\beta P^*$. By writing $P=\alpha P^*+\beta P^* f(t)$ then the matrix equation K_g becomes

$$K_g=\alpha P^*[K_{gs}]+\beta P^*[K_{gt}] \tag{2.13}$$

where the matrices $[K_{gs}]$ and $[K_{gt}]$ reflect the influence of P_o and P_t respectively. Substituting equation (2.13) into equation (2.11), the following system of n second order differential equations with a periodic coefficient of the known Mathieu-Hill type is obtained;

$$[M]\{\ddot{q}\}+\left[[K_e]-\alpha P^*[K_{gs}]-\beta P^* f(t)[K_{gt}]\right]\{q\}=0 \tag{2.14}$$

f(t) is a periodic function with period T. Therefore

$$f(t+T)=f(t) \tag{2.15}$$

Equation (2.14) is a system of n second order differential equations which may be written as

$$\{\ddot{q}(t)\}+[Z]\{q(t)\}=0 \tag{2.16}$$

where

$$[Z]=[M]^{-1}\left[[K_e]-\alpha P^*[K_{gs}]-\beta P^*[K_{gt}]\right] \tag{2.17}$$

It is convenient to replace the n second order equations with 2n first order equations by introducing

$$\{h\}=\begin{Bmatrix} q \\ \dot{q} \end{Bmatrix} \tag{2.18}$$

and

$$[\phi]=\begin{bmatrix} 0 & -[I] \\ [Z] & 0 \end{bmatrix} \tag{2.19}$$

then, equation (2.16) becomes

$$\{\dot{h}(t)\}+[\phi(t)]\{h(t)\}=\begin{Bmatrix} \dot{q} \\ \ddot{q} \end{Bmatrix}+\begin{bmatrix} 0 & -[I] \\ [Z] & 0 \end{bmatrix}\begin{Bmatrix} q \\ \dot{q} \end{Bmatrix}=0 \tag{2.20}$$

Equation (2.19) needs not be solved completely in order to determine the stability of the system. It is merely necessary to determine whether the solution is bounded or unbounded.

It is assumed that the 2n linearly independent solutions of equation (2.20) are known over the interval t = 0 to t = T. Then they may be represented in matrix form as

$$\left[H(t)\right]=\begin{bmatrix} h_{1,1} & . & . & . & h_{1,2n} \\ . & . & . & . & . \\ . & . & . & . & . \\ . & . & . & . & . \\ h_{2n,1} & . & . & . & h_{2n,2n} \end{bmatrix} \tag{2.21}$$

Since f(t), and therefore $\left[\phi(t)\right]$ is periodic with period T, then the substitution t = t + T will not alter the form of the equations, and the matrix solutions, at time t + T, $\left[H(t+T)\right]$ may be obtained from $\left[H(t)\right]$ by a linear transformation

$$\left[H(t+T)\right]=\left[R\right]\left[H(t)\right] \tag{2.22}$$

where $\left[R\right]$ is the transformation matrix and is composed only of constant coefficients.

It is desirable to find a set of solutions for which the matrix $\left[R\right]$ can be diagonalized. Hence the i^{th} solution vector after period T, $\left\{\bar{h}(t+T)\right\}_i$ may be determined from $\left\{\bar{h}(t)\right\}_i$ using the simple expression

$$\left\{\bar{h}(t+T)\right\}_i=\rho_i\left\{\bar{h}(t)\right\}_i \tag{2.23}$$

The behavior of the solution is determined by ρ_i.

If $\rho_i>1$, then the amplitude of vibration will increase with time. If $\rho_i<1$, then the amplitude will decrease. For $\rho_i=1$, the amplitude will remain unchanged, and this represents the stable boundary.

In order to diagonalize the matrix $\left[R\right]$, the characteristic equation

$$\left|\left[R\right]-\rho\left[I\right]\right|=0 \tag{2.24}$$

must be solved for its 2n roots, where $\left[I\right]$ is the identity matrix. The roots of the equations, ρ_i, are eigenvalues, each having a corresponding eigenvector.

The 2n resulting eigenvectors are chosen as the 2n solutions to equation (2.20). They can be placed in a matrix, $\left[\bar{H}(t)\right]$, which will then satisfy the expression

$$\left[\bar{H}(t)\right]=\left[\bar{R}\right]\left[\bar{H}(t+T)\right] \tag{2.25}$$

where

$$\left[\bar{R}\right]=\begin{bmatrix}\rho_1 & 0 & . & . & 0\\ 0 & \rho_2 & . & . & 0\\ . & . & . & . & .\\ . & . & . & . & .\\ 0 & . & . & 0 & \rho_{2n}\end{bmatrix} \tag{2.26}$$

$\left[\bar{R}\right]$ is the diagonalized matrix of $\left[R\right]$ composed of the 2n eigenvalues of equation (2.24).

The periodic vector, $\left\{Z(t)\right\}_i$, with period T is introduced so that

$$\left\{\bar{h}(t)\right\}_i=\left\{Z(t)\right\}_i e^{(t/T)\ln\rho_i} \tag{2.27}$$

For an even function of time like $\left[\phi(t)\right]$, it is true that

$$[\phi(t)]=[\phi(-t)] \tag{2.28}$$

Hence equation (2.27) can be written as

$$\left\{\bar{h}(-t)\right\}_i = \left\{Z(-t)\right\}_i e^{-(t/T)\ln\rho_i} \tag{2.29}$$

then

$$\left\{\bar{h}(-t)\right\}_i = \left\{Z(-t)\right\}_i e^{(t/T)\ln(1/\rho_i)} \tag{2.30}$$

It is clear from (2.30) that $1/\rho_i$ is also an eigenvalue. This property is not restricted to even functions, but is also preserved in the case of arbitrary periodic functions as shown by Bolotin, (1964).

In general, the eigenvalues ρ_i are complex numbers of the form

$$\rho_i = a_i + j b_i \tag{2.31}$$

and the natural logarithm of a complex number is given by

$$\ln\rho_i = \ln|\rho_i| + j \text{ (argument } \rho) \tag{2.32}$$

or in this case

$$\ln\rho_i = \ln\sqrt{a_i^2 + b_i^2} + j\tan^{-1}(b_i / a_i) \tag{2.33}$$

where $j = \sqrt{-1}$

From equation (2.27), it is clear that if the real part of $\log\rho_i$ is positive for any of the solutions, then that solution will be unbounded with time. A negative real part

means that the corresponding solution will damp out with time. It therefore follows that the boundary case for a given solution is that for which the characteristic exponent has a zero real part. This is identical to saying that absolute value of ρ_i is unity. For the system to remain stable, every one of the solutions must remain bounded. If even one of the solutions has a characteristic exponent which is positive, then the corresponding solution is unbounded and therefore the system is unstable.

It has been shown that if ρ_i is a solution, then $1/\rho_i$ is also a solution. These two solutions can be written as

$$\rho_i = a_i + jb_i \tag{2.34}$$

$$\rho_{i+n} = (a_i - jb_i)/(a_i^2 + b_i^2) \tag{2.35}$$

Another restriction on the solutions of the characteristic equation is that the complex eigenvalues must occur in complex conjugate pairs. Hence it follows that ρ_{i+1} and ρ_{i+n+1} are also solutions where

$$\rho_{i+1} = a_i - jb_i \tag{2.36}$$

$$\rho_{i+n+1} = (a_i + jb_i)/(a_i^2 + b_i^2) \tag{2.37}$$

These solutions are presented in figure 2.4 which shows a unit circle in the complex plane. The area inside the unit circle represents stable or bounded solutions, while the area outside the unit circle represents unstable or unbounded solutions. For each stable solution which lies inside the circle, there corresponds an unstable solution outside the circle due to the reciprocity constraint. Therefore the only possible stable solutions must lie on the unit circle.

Points on this unit circle may be represented in polar co-ordinates by r = 1 and $\theta = \tan^{-1}b/a$ where $-\pi \leq \theta \leq \pi$. For each root on the upper semicircle, there is a

corresponding root on the lower semicircle due to the fact that the roots occur in complex conjugate pairs. The logarithm of ρ_i, when ρ_i lies on the unit circle will be

$$\ln \rho_i = j\theta \tag{2.38}$$

and equation (2.27) becomes

$$\left\{\bar{h}(t)\right\}_i = \left\{Z(t)\right\}_i e^{j\left(\frac{\theta t}{T}\right)} \tag{2.39}$$

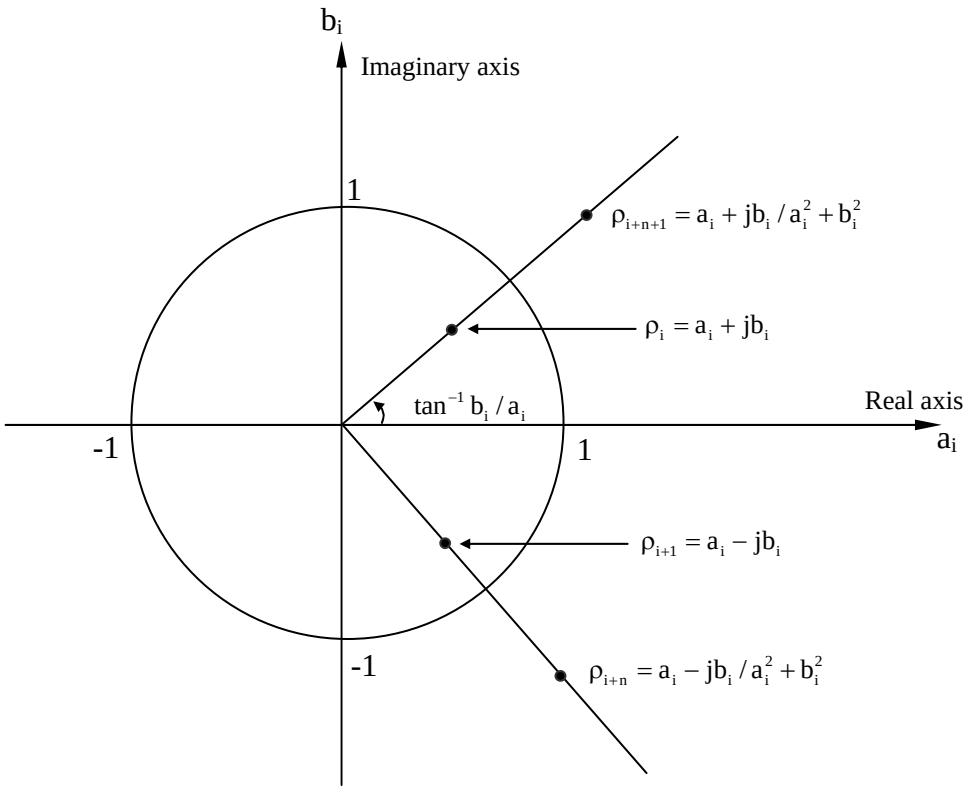

Figure 2.4 Unit circle in the complex plane

Since the eigenvalues occur in complex conjugate pairs, the limiting values of θ are zero and π.

When $\theta = 0$, equation (2.39) becomes

$$\left\{\bar{h}(t)\right\}_i = \left\{Z(t)\right\}_i \tag{2.40}$$

and, therefore, the solution $\left\{\bar{h}(t)\right\}$ is periodic with period T when $\theta = \pi$, equation (2.39) becomes

$$\left\{\bar{h}(t)\right\}_i = \left\{Z(t)\right\}_i e^{j\left(\frac{\pi t}{T}\right)} \tag{2.41}$$

$$\left\{\bar{h}(t+2T)\right\}_i = \left\{Z(t+2T)\right\}_i e^{j\left(\frac{\pi(t+2T)}{T}\right)} = \left\{\bar{h}(t)\right\}_i \tag{2.42}$$

It is clear from equation (2.42) that the solution $\left\{\bar{h}(t)\right\}$ is also periodic with a period 2T.

It can be concluded that equation (2.11) has periodic solutions of period T and 2T. Also the boundaries between stable and unstable regions are formed by periodic solutions of period T and 2T.

For a system subjected to the periodic force

$$P = P_0 + P_t \cos \omega t \tag{2.43}$$

Where ω is the disturbing frequency, equation (2.11) becomes

$$\left[M\right]\left\{\ddot{q}\right\} + \left[\left[K_e\right] - \alpha P^* \left[K_{gs}\right] - \beta P^* \cos \omega t \left[K_{gt}\right]\right]\left\{q\right\} = 0 \tag{2.44}$$

Now we seek periodic solutions of period T and 2T of equation (2.44) where $T = 2\pi/\omega$.

When a solution of period 2T exists, it may be represented by the Fourier series

$$\{q\} = \sum_{k=1,3,5}^{\infty} \left[\{a\}_k \sin\frac{k\omega t}{2} + \{b\}_k \cos\frac{k\omega t}{2} \right] \tag{2.45}$$

Where $\{a\}_k$ and $\{b\}_k$ are time-independent vectors. Differentiating equation (2.45) twice with respect to time yields

$$\{\ddot{q}\} = \sum_{k=1,3,5}^{\infty} -\left(\frac{k\omega}{2}\right)^2 \left[\{a\}_k \sin\frac{k\omega t}{2} + \{b\}_k \cos\frac{k\omega t}{2} \right] \tag{2.46}$$

Substituting equations (2.45) and (2.46) into equation (2.44) and using the trigonometric relations

$$\begin{aligned}
&\sin A + \sin B = 2 \sin\frac{A+B}{2} \cos\frac{A-B}{2} \\
&\sin A - \sin B = 2 \cos\frac{A+B}{2} \sin\frac{A-B}{2} \\
&\cos A + \cos B = 2 \cos\frac{A+B}{2} \cos\frac{A-B}{2} \\
&\cos A - \cos B = 2 \sin\frac{A+B}{2} \sin\frac{A-B}{2}
\end{aligned} \tag{2.47}$$

and comparing the coefficients of $\sin\frac{k\omega t}{2}$ and $\cos\frac{k\omega t}{2}$ lead to the following matrix equations relating the vectors $\{a\}_k$ and $\{b\}_k$.

$$\begin{bmatrix}
[K_e] - \alpha P^*[K_{gs}] + \frac{1}{2}\beta P^*[K_{gt}] - \frac{\omega^2}{4}[M] & -\frac{1}{2}\beta P^*[K_{gt}] & 0 & . \\
-\frac{1}{2}\beta P^*[K_{gt}] & [K_e] - \alpha P^*[K_{gs}] - \frac{9\omega^2}{4}[M] & -\frac{1}{2}\beta P^*[K_{gt}] & . \\
0 & -\frac{1}{2}\beta P^*[K_{gt}] & [K_e] - \alpha P^*[K_{gs}] - \frac{25\omega^2}{4}[M] & . \\
. & . & . & .
\end{bmatrix} \begin{Bmatrix} \{a\}_1 \\ \{a\}_3 \\ \{a\}_5 \\ . \end{Bmatrix} = 0$$

(2.48)

and

$$\begin{bmatrix} [K_e]-\alpha P^*[K_{gs}]-\frac{1}{2}\beta P^*[K_{gt}]-\frac{\omega^2}{4}[M] & -\frac{1}{2}\beta P^*[K_{gt}] & 0 & . \\ -\frac{1}{2}\beta P^*[K_{gt}] & [K_e]-\alpha P^*[K_{gs}]-\frac{9\omega^2}{4}[M] & -\frac{1}{2}\beta P^*[K_{gt}] & . \\ 0 & -\frac{1}{2}\beta P^*[K_{gt}] & [K_e]-\alpha P^*[K_{gs}]-\frac{25\omega^2}{4}[M] & . \\ . & . & . & . \end{bmatrix} \begin{Bmatrix} \{b\}_1 \\ \{b\}_3 \\ \{b\}_5 \\ . \end{Bmatrix} = 0$$

(2.49)

The orders of matrices in equations (2.48) and (2.49) are infinite. If solutions of period 2T exist, then the determinants of these matrices must zero. Combining these two determinants, the condition may be written as

$$\begin{vmatrix} [K_e]-\alpha P^*[K_{gs}]\pm\frac{1}{2}\beta P^*[K_{gt}]-\frac{\omega^2}{4}[M] & -\frac{1}{2}\beta P^*[K_{gt}] & 0 & . \\ -\frac{1}{2}\beta P^*[K_{gt}] & [K_e]-\alpha P^*[K_{gs}]-\frac{9\omega^2}{4}[M] & -\frac{1}{2}\beta P^*[K_{gt}] & . \\ 0 & -\frac{1}{2}\beta P^*[K_{gt}] & [K_e]-\alpha P^*[K_{gs}]-\frac{25\omega^2}{4}[M] & . \\ . & . & . & . \end{vmatrix} = 0$$

(2.50)

If a solution to equation (2.44) exists with a period $T=2\pi/\omega$ then it may be expressed as Fourier series

$$\{q\} = \frac{1}{2}b_0 + \sum_{k=2,4,6}^{\infty}\left[\{a\}_k \sin\frac{k\omega t}{2} + \{b\}_k \sin\frac{k\omega t}{2}\right] \qquad (2.51)$$

Differentiating equation (2.51) twice with respect to time yields

$$\{\ddot{q}\} = \sum_{k=2,4,6}^{\infty} -\left(\frac{k\omega}{2}\right)^2\left[\{a\}_k \sin\frac{k\omega t}{2} + \{b\}_k \cos\frac{k\omega t}{2}\right] \qquad (2.52)$$

Substituting equations (2.51) and (2.52) into equation (2.44), the following condition for the existence of solution with period T is obtained;

$$\begin{bmatrix} [K_e]-\alpha P^*[K_{gs}]-\omega^2[M] & -\frac{1}{2}\beta P^*[K_{gt}] & 0 & . \\ -\frac{1}{2}\beta P^*[K_{gt}] & [K_e]-\alpha P^*[K_{gs}]-4\omega^2[M] & -\frac{1}{2}\beta P^*[K_{gt}] & . \\ 0 & -\frac{1}{2}\beta P^*[K_{gt}] & [K_e]-\alpha P^*[K_{gs}]-9\omega^2[M] & . \\ . & . & . & . \end{bmatrix} \begin{Bmatrix} \{a\}_2 \\ \{a\}_4 \\ \{a\}_6 \\ . \end{Bmatrix} = 0 \tag{2.53}$$

and

$$\begin{bmatrix} \frac{1}{2}\{[K_e]-\alpha P^*[K_{gs}]\} & -\frac{1}{2}\beta P^*[K_{gt}] & 0 & 0 & . \\ -\frac{1}{2}\beta P^*[K_{gt}] & [K_e]-\alpha P^*[K_{gs}]-\omega^2[M] & -\frac{1}{2}\beta P^*[K_{gt}] & 0 & . \\ 0 & -\frac{1}{2}\beta P^*[K_{gt}] & [K_e]-\alpha P^*[K_{gs}]-4\omega^2[M] & -\frac{1}{2}\beta P^*[K_{gt}] & . \\ 0 & & -\frac{1}{2}\beta P^*[K_{gt}] & [K_e]-\alpha P^*[K_{gs}]-9\omega^2[M] & . \\ 0 & . & . & . & . \end{bmatrix} \begin{Bmatrix} \{b\}_0 \\ \{b\}_2 \\ \{b\}_4 \\ \{b\}_6 \\ . \\ . \end{Bmatrix} = 0 \tag{2.54}$$

It has been shown by Bolotin (1964), that solutions with period 2T are the ones of the greatest practical importance and that as a first approximation the boundaries of the principal regions of dynamic instability can be determined from the equation

$$\left[[K_e]-\alpha P^*[K_{gs}] \pm \frac{1}{2}\beta P^*[K_{gt}] - \frac{\omega^2}{4}[M]\right]\{q\} = 0 \tag{2.55}$$

The two matrices $[K_{gs}]$ and $[K_{gt}]$ will be identical if the static and time dependent components of the loads are applied in the same manner. If $[K_{gs}] \equiv [K_{gt}] \equiv [K_g]$, then equation (2.56) becomes

$$\left[\left[K_e\right]-(\alpha\pm\frac{1}{2}\beta)P*\left[K_g\right]-\frac{\omega^2}{4}\left[M\right]\right]\{q\}=0 \tag{2.56}$$

Equation (2.56) represents solutions to three related problems

(i) Free vibration with $\alpha = 0$, $\beta = 0$ and $p = \omega/2$ the natural frequency

$$\left[\left[K_e\right]-p^2\left[M\right]\right]\{q\}=0 \tag{2.57}$$

(ii) Static stability with $\alpha = 1$, $\beta = 0$ and $\omega = 0$

$$\left[\left[K_e\right]-P*\left[K_g\right]\right]\{q\}=0 \tag{2.58}$$

(iii) Dynamic stability when all terms are present

$$\left[\left[K_e\right]-(\alpha\pm\frac{1}{2}\beta)P*\left[K_g\right]-\frac{\omega^2}{4}\left[M\right]\right]\{q\}=0 \tag{2.59}$$

CHAPTER THREE
NUMERICAL METHOD

3.1 The Finite Element Method

3.1.1 What is the Finite Element Method?

The finite element method is a numerical analysis technique for obtaining approximate solutions to a wide variety of engineering problems. Although originally developed to study the stresses in complex airframe structures, it has since been extended and applied to the broad field of continuum mechanics. Because of its diversity and flexibility as an analysis tool, it is receiving much attention in engineering schools and in industry.

In more and more engineering situations today, we find that it is necessary to obtain approximate numerical solutions to problems rather than exact closed-form solutions. For example, we may want to find the load capacity of a plate that has several stiffeners and odd-shaped holes, the concentration of pollutants during non-uniform atmospheric conditions or the rate of fluid flow through a passage of arbitrary shape. Without too much effort, we can write down the governing equations and boundary conditions for these problems, but we see immediately that no simple analytical solution can be found. The difficulty in these three examples lies in the fact that either the geometry or some other feature of the problem is irregular or "arbitrary." Analytical solutions to problems of this type seldom exist; yet these are the kinds of problems that engineers and scientists are called upon to solve.

The resourcefulness of the analyst usually comes to the rescue and provides several alternatives to overcome this dilemma. One possibility is to make simplifying assumptions-to ignore the difficulties and reduce the problem to one that can be handled. Sometimes this procedure works; but, more often than not, it leads to serious inaccuracies or wrong answers. Now that large-scale digital computers are

Several approximate numerical analysis methods have evolved over the years-the most commonly used method is the general finite difference scheme. The familiar finite difference model of a problem gives a pointwise approximation to the governing equations. This model (formed by writing difference equations for an array of grid points) is improved as more points are used. With finite difference techniques we can treat some fairly difficult problems; but, for example, when we encounter irregular geometries or an unusual specification of boundary conditions, we find that finite difference techniques become hard to use.

In addition to the finite difference method, another, more recent numerical method (known as the "finite element method") has emerged. Unlike the finite difference method, which envisions the solution region as an array of grid points, the finite element method envisions the solution region as built up of many small, interconnected sub-regions or elements. A finite element model of a problem gives a piece-wise approximation to the governing equations. The basic premise of the finite element method is that a solution region can be analytically modeled or approximated by replacing it with an assemblage of discrete elements. Since these elements can be put together in a variety of ways, they can be used to represent exceedingly complex shapes.

As an example of how a finite difference model and a finite element model might be used to represent a complex geometrical shape, consider the turbine blade cross section in Figure 3.1. For this device we may want to find the distribution of displacements and stresses for a given force loading or the distribution of temperature for a given thermal loading. The interior coolant passage of the blade, along with its exterior shape, gives it a non-simple geometry.

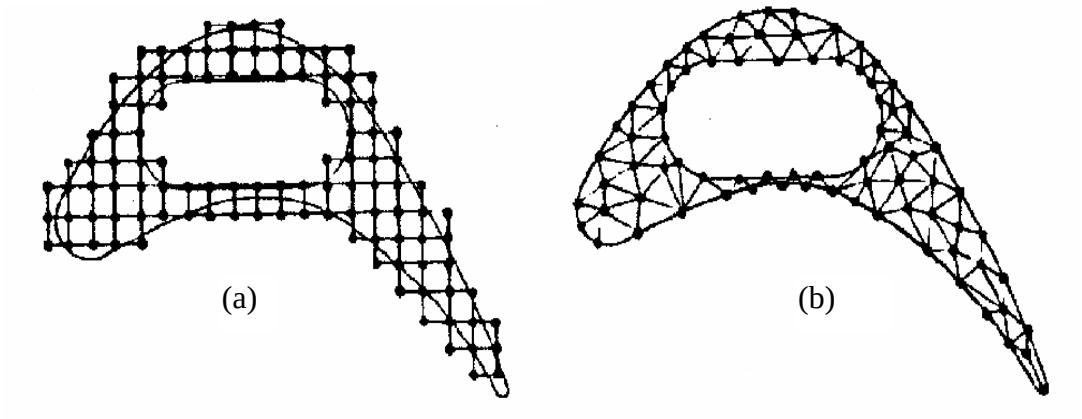

Figure 3.1 Finite difference and finite element discretizations of a turbine blade profile. (a) Typical finite difference model. (b) Typical finite element model.

A uniform finite difference mesh would reasonably cover the blade (the solution region), but the boundaries must be approximated by a series of horizontal and vertical lines (or "stair steps"). On the other hand, the finite element model (using the simplest two-dimensional element- the triangle) gives a better approximation to the region and requires fewer nodes. Also, a better approximation to the boundary shape results because the curved boundary is represented by a series of straight lines. This example is not intended to suggest that finite element models are decidedly better than finite difference models for all problems. The only purpose of the example is to demonstrate that the finite element method is particularly well suited for problems with complex geometries.

3.1.2 How the Method Works

We have been alluding to the essence of the finite element method, but now we shall discuss it in greater detail. In a continuum problem of any dimension the field variable (whether it is pressure, temperature, displacement, stress or some other quantity) possesses infinitely many values because it is a function of each generic point in the body or solution region. Consequently, the problem is one with an infinite number of unknowns. The finite element discretization procedures reduce the problem to one of a finite number of unknowns by dividing the solution region into

elements and by expressing the unknown field variable in terms of assumed approximating functions within each element. The approximating functions (sometimes called interpolation line functions) are defined in terms of the values of the field variables at specified points called nodes or nodal points. Nodes usually lie on the element boundaries where adjacent elements are considered to be connected. In addition to boundary nodes, an element may also have a few interior nodes. The nodal values of the field variable and the interpolation functions for the elements completely define the behavior of the field variable within the elements. For the finite element representation of a problem the nodal values of the field variable become the new unknowns. Once these unknowns are found, the interpolation functions define the field variable throughout the assemblage of elements.

Clearly, the nature of the solution and the degree of approximation depend not only on the size and number of the elements used, but also on the interpolation functions selected. As one would expect, we cannot choose functions arbitrarily, because certain compatability conditions should be satisfied. Often functions are chosen so that the field variable or its derivatives are continuous across adjoining element boundaries.

Thus far we have briefly discussed the concept of modeling an arbitrarily shaped solution region with an assemblage of discrete elements and we have pointed out that interpolation functions must be defined for each element. We have not yet mentioned, however, an important feature of the finite element method that sets it apart from other approximate numerical methods. This feature is the ability to formulate solutions for individual elements before putting them together to represent the entire problem. This means, for example, that if we are treating a problem in stress analysis, we can find the force-displacement or stiffness characteristics of each individual element and then assemble the elements to find the stiffness of the whole structure. In essence, a complex problem reduces to considering a series of greatly simplified problems.

Another advantage of the finite element method is the variety of ways in which one can formulate the properties of individual elements. There are basically four different approaches. The first approach to obtaining element properties is called the direct approach because its origin is traceable to the direct stiffness method of structural analysis. The direct approach also suggests the need for matrix algebra in dealing with the finite element equations.

Element properties obtained by the direct approach can also be determined by the more versatile and more advanced variational approach. The variational approach relies on the calculus of variations and involves extremizing a functional. For problems in solid mechanics the functional turns out to be the potential energy, the complementary potential energy or some derivative of these, such as the Reissner variational principle. Knowledge of the variational approach is necessary to work beyond the introductory level and to extend the finite element method to a wide variety of engineering problems. Whereas the direct approach can be used to formulate element properties for only the simplest element shapes, the variational approach can be employed for both simple and sophisticated element shapes.

A third and even more versatile approach to deriving element properties has its basis entirely in mathematics and is known as the weighted residuals approach. The weighted residuals approach begins with the governing equations of the problem and proceeds without relying on a functional or a variational statement. This approach is advantageous because it thereby becomes possible to extend the finite element method to problems where no functional is available. For some problems we do not have a functional-either because one may not have been discovered or because one does not exist.

A fourth approach relies on the balance of thermal and/or mechanical energy of a system. The energy balance approach (like the weighted residuals approach) requires no variational statement and hence broadens considerably the range of possible applications of the finite element method.

Regardless of the approach used to find the element properties, the solution of a continuum problem by the finite clement method always follows an orderly step-by-step process.

1. Discretize the Continuum. The first step is to divide the continuum or solution region into elements. In the example of Figure 3.1 the turbine blade has been divided into triangular elements that might be used to find the temperature distribution or stress distribution in the blade. A variety of element shapes may be used and with care, different element shapes may be employed in the same solution region. Indeed, when analyzing an elastic structure that has different types of components such as plates and beams, it is not only desirable but also necessary to use different types of elements in the same solution. Although the number and the type of elements to be used in a given problem are matters of engineering judgment, the analyst can rely on the experience of others for guidelines.

2. Select interpolation functions. The next step is to assign nodes to each element and then choose the type of interpolation function to represent the variation of the field variable over the element. The field variable may be a scalar, a vector or a higher-order tensor. Often, although not always, polynomials are selected as interpolation functions for the field variable because they are easy to integrate and differentiate. The degree of the polynomial chosen depends on the number of nodes assigned to the element, the nature and number of unknowns at each node and certain continuity requirements imposed at the nodes and along the element boundaries. The magnitude of the field variable as well as the magnitude of its derivatives may be the unknowns at the nodes.

3. Find the element properties. Once the finite element model has been established (that is, once the elements and their interpolation functions have been selected), we are ready to determine the matrix equations expressing the properties of the individual elements. For this task we may use one of the four approaches just mentioned: the direct approach, the variational approach, the weighted residual approach or the energy balance approach. The variational approach is often the most

convenient, but for any application the approach used depends entirely on the nature of the problem.

4. Assemble the element properties to obtain the system equations. To find the properties of the overall system modeled by the network of elements we must “assemble” all the element properties. In other words, we must combine the matrix equations expressing the behavior of the elements and form the matrix equations expressing the behavior of the entire solution region or system. The matrix equations for the system have the same form as the equations for an individual element except that they contain many more terms because they include all nodes.

The basis for the assembly procedure stems from the fact that at a node, where elements are interconnected, the value of the field variable is the same for each element sharing that node. Assembly of the element equations is a routine matter in the finite element analysis and is usually done by a digital computer.

Before the system equations are ready for solution they must be modified to account for the boundary conditions of the problem.

5. Solve the system equations. The assembly process of the preceding step gives a set of simultaneous equations that we can solve to obtain the unknown nodal values of the field variable.

6. Make additional computations if desired. Sometimes we may want to use the solution of the system equations to calculate other important parameters. For example, in a fluid mechanics problem such as the lubrication problem, the solution of the system equations gives the pressure distribution within the system. From the nodal values of the pressure we may then calculate velocity distributions and flows or perhaps shear stresses if these are desired.

3.1.3 Range of Applications

Applications of the finite element method can be divided into three categories, depending on the nature of the problem to be solved. In the first category are all the problems known as equilibrium problems or time-independent problems. The majority of applications of the finite element method fall into this category. For the solution of equilibrium problems in the solid mechanics area we need to find the displacement distribution or the stress distribution or perhaps the temperature distribution for a given mechanical or thermal loading. Similarly, for the solution of equilibrium problems in fluid mechanics, we need to find pressure, velocity, temperature and sometimes concentration distributions under steady-state conditions.

In the second category are the so-called eigenvalue problems of solid and fluid mechanics. These are steady-state problems whose solution often requires the determination of natural frequencies and modes of vibration of solids and fluid. Examples of eigenvalue problems involving both solid and fluid mechanics appear in civil engineering when the interaction of lakes and dams is considered and in aerospace engineering when the surge of liquid fuels in flexible tanks is involved. Another class of eigenvalue problems includes the stability of structures and the stability of laminar flows.

In the third category is the multitude of time-dependent or propagation problems of continuum mechanics. This category is composed of the problems that result when the time dimension is added to the problems of the first two categories.

Just about every branch of engineering is a potential user of the finite element method. But the mere fact that this method can be used to solve a particular problem does not mean that it is the most practical solution technique. Often several attractive techniques are available to solve a given problem. Each technique has its relative merits and no technique enjoys the lofty distinction of being “the best” for all problems. Consequently, when a designer or analyst has a continuum problem to solve, his first major step is to decide which method to use. This involves a study of

the alternative methods of solution, the availability of computer facilities and computer packages and most important of all, the amount of time and money that can be spent to obtain a solution.

The range of possible applications of the finite element method extends to all engineering disciplines, but civil and aerospace engineers concerned with stress analysis are the most frequent users of the method. Major aircraft companies and other organizations involved in the design of structures have developed elaborate finite element computer programs.

CHAPTER FOUR
THEORETICAL ANALYSIS

The vibration problem of curved beams has been the subject of interest of several investigators due to its importance in many practical applications.

4.1 The Finite Element Model of a Curved Beam without Internal Node

4.1.1 Mathematical Model

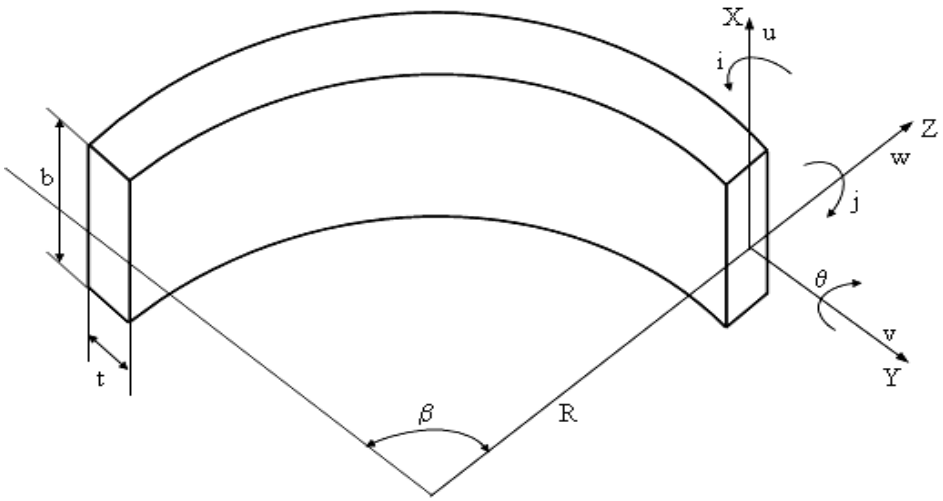

Figure 4.1 Coordinate system and displacements of the curved beam finite element

The out- of –plane vibration for horizontally curved beam shown in figure 3.1 is considered. As it may be seen, R denotes the radius of curvature at the centroid, b and t are the width and height of the section and β is the angle between outer supports. Also, it may be seen in figure 4.1 that a right – hand co-ordinate system is used. Axes x and z principal centiroid axes of the beam cross-section and y is the tangent to the curved axis of this member.

4.1.2 Theoretical Consideration

The out-of-plane curved beam element used in this analysis is given by Belek, (1977) and is based on strain functions. The strain displacement equations are integrated by making an assumption of uniform torsional strain and linear increase in curvature.

Deflection functions used in the analysis are given by Belek, (1977) as

$$u = a_1 R\cos\phi + a_2 R\sin\phi + a_3 R - a_4 R\phi - a_6 R\phi$$

$$\theta = a_1\cos\phi + a_2\sin\phi - a_5 - a_6\phi, \qquad \phi = y/R \tag{4. 1}$$

4.1.3 Strain energy of out-of-plane vibration of a curved beam

The strain energy of a curved beam under coupled bending and torsional displacements is in given by Belek, (1977) as,

$$V_o = \int_0^{l_{sh}} \left[E_s I_{yys}\left(u'' + \frac{\theta}{R} \right)^2 + G_s J_{xxs}\left(\theta' - \frac{u'}{R} \right)^2 \right] dy \tag{4.2}$$

By substituting equation 4.1 in to equation 4.2 if becomes,

$$V_0 = \frac{1}{2}\{q_0\}^T [C_0]^{-T} \left\{ \int_0^{l_{sh}} \begin{bmatrix} \theta/R + u'' \\ \theta' - u'/R \end{bmatrix} \begin{bmatrix} E_s I_{yys} & 0 \\ 0 & G_s J_{xxs} \end{bmatrix} \begin{bmatrix} \theta/R + u'' \\ \theta' - u'/R \end{bmatrix} dy \right\} [C_0]^{-1} \{q_0\} \tag{4.3}$$

$$V_o = \frac{1}{2}\{q_o\}^T [C_o]^{-T} [k_o][C_o]^{-1} \{q_o\} \tag{4. 4}$$

Where $\{q_0\}^T, [C_0]^{-1}, [k_o]$ are given explicitly in equation (4.5), (4.6) and (4.7) respectively.

$$\{q_o\}^T = [\theta_i \;\; u_i \;\; j_i \;\; \theta_{i+1} \;\; u_{i+1} \;\; j_{i+1}] \qquad j = -\frac{\partial u}{\partial y} \tag{4. 5}$$

the stiffness matrix $[k_0]$ is given by

$$[k_o] = \frac{E_s I_{yys}}{R} \begin{bmatrix} 0 & 0 & 0 & 0 & 0 & 0 \\ & 0 & 0 & 0 & 0 & 0 \\ & & 0 & 0 & 0 & 0 \\ & & & C_2\beta & 0 & 0 \\ & & & & \beta & \beta^2/2 \\ & & & & & \beta^3/3 \end{bmatrix} \tag{4. 6}$$

$$C_2 = \frac{G_s J_{xxs}}{E_s I_{yys}}$$

and the transformation matrix $[C_o]^{-1}$ is given by

$$[C_o]^{-1} = \begin{bmatrix} 0 & -B_{o1}/R & B_{o2} & 0 & B_{o1}/R & B_{o3} \\ 0 & -B_{o5}/R & -B_{o4} & 0 & B_{o5}/R & -B_{o1} \\ 0 & B_{o4}/R & -B_{o2} & 0 & -B_{o1}/R & -B_{o3} \\ -1/\beta & 1/(R\,\beta) & 0 & 1/\beta & -1/(R\,\beta) & 0 \\ -1 & -B_{o1}/R & B_{o2} & 0 & B_{o1}/R & B_{o3} \\ 1/\beta & 2B_{o1}/(R\,\beta) & -B_{o1} & -1/\beta & -2B_{o1}/(R\,\beta) & -B_{o1} \end{bmatrix} \tag{4. 7}$$

$$D_o = 2 - 2\cos\beta - \beta\sin\beta$$

$$B_{o1} = (\cos\beta - 1)/D_o$$

$$B_{o2} = \sin\beta / D_o$$

$$B_{o3} = (\sin\beta - \beta)/D_o$$

$$B_{o4} = (1 - \cos\beta - \beta\sin\beta)/D_o$$

$$B_{o5} = \sin\beta / D_o$$

4.1.4 External work done in the out-of-plane direction of a curved beam due to uniform in-plane compression forces

External work will be done in the out of plane direction when the shroud is subjected to uniform compression force P(t).The additional energy V_{gc} due to periodic force (Papangelis & Trahair, 1987)

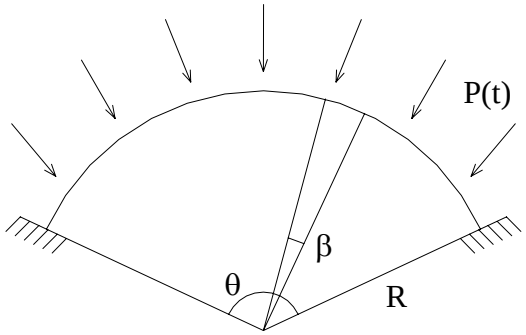

Figure 4.2 Curved beam subjected to uniform compression force

$$V_{go} = \int_0^{l_{sh}} P(t)R\left[u'^2 + r_x^2\theta'^2 + r_y^2(\theta' - \frac{u'}{R})^2 \right] dy \qquad (4.\ 8)$$

where,

$$r_x^2 = \frac{I_{xxs}}{A_s}, \qquad r_y^2 = \frac{I_{yys}}{A_s} \qquad (4.\ 9)$$

By substituting equation 4.1 in to equation 4.8

$$V_{go} = \frac{1}{2}\{q_o\}^T [C_o]^{-T} [k_{go}] [C_o]^{-1} \{q_o\} \qquad (4.\ 10)$$

$$g_1 = \begin{bmatrix} \sin^2\theta & -\sin\theta\cos\theta & 0 & \sin\theta & 0 & \sin\theta \\ & \cos^2\theta & 0 & -\cos\theta & 0 & -\cos\theta \\ & & 0 & 0 & 0 & 0 \\ & & & 1 & 0 & 1 \\ & & & & 0 & 0 \\ & & & & & 1 \end{bmatrix} \tag{4.11.a}$$

$$g_2 = \begin{bmatrix} \sin^2\theta & -\sin\theta\cos\theta & 0 & 0 & 0 & \sin\theta \\ & \cos^2\theta & 0 & 0 & 0 & -\cos\theta \\ & & 0 & 0 & 0 & 0 \\ & & & 0 & 0 & 0 \\ & & & & 0 & 0 \\ & & & & & 1 \end{bmatrix} \tag{4.11.b}$$

$$g_3 = \begin{bmatrix} -\sin^2\theta & \sin\theta\cos\theta & 0 & -\sin\theta & 0 & -\sin\theta \\ \sin\theta\cos\theta & -\cos^2\theta & 0 & \cos\theta & 0 & \cos\theta \\ 0 & 0 & 0 & 0 & 0 & 0 \\ 0 & 0 & 0 & 0 & 0 & 0 \\ 0 & 0 & 0 & 0 & 0 & 0 \\ -\sin\theta & \cos\theta & 0 & -1 & 0 & -1 \end{bmatrix} \tag{4.11.c}$$

$$g_4 = \begin{bmatrix} -\sin^2\theta & \sin\theta\cos\theta & 0 & 0 & 0 & -\sin\theta \\ \sin\theta\cos\theta & -\cos^2\theta & 0 & 0 & 0 & \cos\theta \\ 0 & 0 & 0 & 0 & 0 & 0 \\ -\sin\theta & \cos\theta & 0 & 0 & 0 & -1 \\ 0 & 0 & 0 & 0 & 0 & 0 \\ -\sin\theta & \cos\theta & 0 & 0 & 0 & -1 \end{bmatrix} \tag{4.11.d}$$

Using the above matrices the matrix $\left[k_{go}\right]$ is obtained

$$\left[KG\right] = \left[R^2 g_1 + r_x^2 g_2 + r_y^2 (g_1 + g_2 + g_3 + g_4)\right] \tag{4.12}$$

$$\left[k_{go}\right]=\int_0^{\beta}\left[KG\right]d\theta \tag{4.13}$$

4.1.5 Kinetic energy of out-of-plane vibration of a curved beam

The kinetic energy expression of a curved beam under combined bending-torsional displacements is given by Belek, (1977) as,

$$T_o = \int_0^{l_{sh}}\left[\rho_s A_s\left(\dot{u}\right)^2+\rho_s I_p\left(\dot{\theta}\right)^2\right]dy \tag{4.14}$$

$$T=\frac{1}{2}\left\{q_0\right\}^T\left[C_0\right]^{-T}\left\{\int_0^{l_{sh}}\begin{bmatrix}u'\\ \theta' R\end{bmatrix}\begin{bmatrix}\rho_s A_s & 0\\ 0 & I_p\rho_s\end{bmatrix}\begin{bmatrix}u'\\ \theta' R\end{bmatrix}dy\right\}\left[C_0\right]^{-1}\left\{q_0\right\} \tag{4.15}$$

By substituting equation 4.1 in to equation 4.15 if becomes,

$$T_o=\frac{1}{2}\left\{\dot{q}_o\right\}^T\left[C_o\right]^{-T}\left[m_o\right]\left[C_o\right]^{-1}\left\{\dot{q}_o\right\} \tag{4.16}$$

Where the corresponding degrees of freedom $\left\{q_o\right\}^T$ and the transformation matrix $\left[C_o\right]^{-1}$ have been given in equations (4.5) and (4.6) respectively and the mass matrix $\left[m_o\right]$ is

$$\left[m_o\right]=\rho_s A_s R^3\begin{bmatrix} C_4M_1 & C_4M_2 & \sin\beta & M_3 & -C_3\sin\beta & C_4M_3\\ & C_4M_4 & M_5 & M_6 & -C_3M_5 & C_4M_6\\ & & \beta & -\beta^2/2 & 0 & -\beta^2/2\\ & & & \beta^3/3 & 0 & \beta^3/3\\ & & & & C_3\beta & C_3\beta^2/2\\ & & & & & C_4\beta^3/3\end{bmatrix} \tag{4.17}$$

$$M_1 = \beta/2 + \sin 2\beta/4$$

$$M_2 = \sin^2 \beta/2$$

$$M_3 = 1 - \cos\beta - \beta\sin\beta$$

$$M_4 = \beta/2 - \sin 2\beta/4$$

$$M_5 = 1 - \cos\beta$$

$$C_3 = \frac{I_p}{(A_s R^2)}$$

$$C_4 = 1 + C_3$$

4.2 The Finite Element Model of a Curved Beam with Internal Node

Deflection functions for the out-of-plane direction of a curved beam element with an internal node used in this analysis are given by Sabuncu (1978).

$$u = a_1 R\cos\phi + a_2 R\sin\phi + a_3 R - a_4 R\phi - a_5 R(1 - \frac{\phi^2}{2}) - a_7 R\phi + a_8 R\left(2 - \phi^2\right) + a_9 R\left(6\phi - \phi^3\right)$$

$$\theta = a_1\cos\phi + a_2\sin\phi + a_5 - a_6 - a_7\phi + a_8\left(2 - \phi^2\right) + a_9\left(6\phi - \phi^3\right), \qquad \phi = {}^{y}\!/_{R} \tag{4.18}$$

4.2.1 Stiffness matrix of out-of-plane vibration of a curved beam

If equation 4.18 is substituted into the strain energy equations 4.2, 4.3 and 4.4, the stiffness matrix is obtained as,

$$[k_0]=\begin{bmatrix} 0 & 0 & 0 & 0 & 0 & 0 & 0 & 0 & 0 \\ & 0 & 0 & 0 & 0 & 0 & 0 & 0 & 0 \\ & & 0 & 0 & 0 & 0 & 0 & 0 & 0 \\ & & & F1\beta & \frac{1}{2}F1\beta^2 & 0 & 0 & 0 & 0 \\ & & & & \frac{1}{3}F1\beta^3 & 0 & 0 & 0 & 0 \\ & & & & & F2\beta & \frac{1}{2}F2\beta^2 & \frac{1}{3}F2\beta^3 & \frac{1}{4}F2\beta^4 \\ & & & & & & \frac{1}{3}F2\beta^3 & \frac{1}{4}F2\beta^4 & \frac{1}{5}F2\beta^5 \\ & & & & & & & \frac{1}{5}F2\beta^5 & \frac{1}{6}F2\beta^6 \\ & & & & & & & & \frac{1}{7}F2\beta^7 \end{bmatrix} \qquad (4.19)$$

where

$$F1=\frac{G_s J_{xxs}}{R}$$

$$F2=\frac{E_s I_{yys}}{R}$$

$$\{q_o\}^T=[\theta_i \;\; u_i \;\; j_i \;\; \theta_{id} \;\; u_{id} \;\; j_{id} \;\; \theta_{i+1} \;\; u_{i+1} \;\; j_{i+1}] \qquad j=-\frac{\partial u}{\partial y} \qquad (4.20)$$

$$[C]=\begin{bmatrix} R & 0 & R & 0 & R & 0 & 0 & 2R & 0 \\ 0 & -1 & 0 & 1 & 0 & 0 & 1 & 0 & -6 \\ 1 & 0 & 0 & 0 & 1 & -1 & 0 & 2 & 0 \\ R\cos(\beta/2) & R\sin(\beta/2) & R & -R\beta/2 & R(1-\beta^2/8) & 0 & -R\beta/2 & R(2-\beta^2/4) & R(3\beta-\beta^3/8) \\ \sin(\beta/2) & -\cos(\beta/2) & 0 & 1 & \beta/2 & 0 & 1 & \beta & -(6-3\beta^2/4) \\ \cos(\beta/2) & \sin(\beta/2) & 0 & 0 & 1 & -1 & -\beta/2 & R(2-\beta^2/4) & (3\beta-\beta^3/8) \\ R\cos(\beta) & R\sin(\beta) & R & -R\beta & R(1-\beta^2/2) & 0 & -R\beta & R(2-\beta^2) & R(6\beta-\beta^3) \\ \sin(\beta) & -\cos(\beta) & 0 & 1 & \beta & 0 & 1 & 2\beta & -(6-3\beta^2) \\ \cos(\beta) & \sin(\beta) & 0 & 0 & 1 & -1 & -\beta & (2-\beta^2) & (6\beta-\beta^3) \end{bmatrix}$$

(4.21)

4.2.2 Geometric stiffness matrix of out-of-plane vibration of a curved beam

When equation 4.18 is substituted into the strain energy equation 4.13, the geometric stiffness matrix is obtained as,

$$[kg]=\begin{bmatrix}
R^2BG1+\frac{Ixxs}{A_S}BG1 & R^2B+\frac{Ixxs}{A_S}B1 & 0 & R^2B2 & R^2BG2 & 0 & R^2B2+\frac{Ixxs}{A_S}B2 & 2R^2BG2-2\frac{Ixxs}{A_S}BG2 & 3R^2BG3+3\frac{Ixxs}{A_S}BG3 \\
 & R^2BG1+\frac{Ixxs}{A_S}BG1 & 0 & -R^2\sin\beta & R^2BG4 & 0 & -R^2\sin\beta-\frac{Ixxs}{A_S}\sin\beta & 2R^2BG4+2\frac{Ixxs}{A_S}BG4 & 3R^2BG5+3\frac{Ixxs}{A_S}BG5 \\
 & & 0 & 0 & 0 & 0 & 0 & 0 & 0 \\
 & & & R^2\beta+\frac{Ixxs}{A_S}\beta & \frac{R^2\beta}{2}+\frac{Ixxs}{2A_S}\beta & 0 & R^2\beta & R^2\beta^2 & R^2(-6\beta+\beta^3) \\
 & & & & \frac{R^2\beta^3}{3}+\frac{Ixxs}{3A_S}\beta^3 & 0 & R^2\beta^2 & \frac{2R^2\beta^3}{3} & R^2(\frac{3}{4}\beta\wedge4-3\beta^2) \\
 & & & & & 0 & 0 & 0 & 0 \\
 & & & & & & R^2\beta+\frac{Ixxs}{A_S}\beta & R^2\beta^2+\frac{Ixxs}{A_S}\beta^2 & R^2(-6\beta+\beta^3)+R^2\frac{Ixxs}{A_S}(\frac{1}{R^2}\beta^3-\frac{6}{R^2}\beta) \\
 & & & & & & & \frac{4}{3}R^2\beta^3+\frac{4}{3}\frac{Ixxs}{A_S}\beta^3 & R^2(\frac{3}{2}\beta^4-6\beta^2)+R^2\frac{Ixxs}{A_S}(\frac{3}{2R^2}\beta^4-\frac{6}{R^2}\beta^2) \\
 & & & & & & & & R^2(\frac{9}{5}\beta^5-12\beta^3+36\beta)+R^4\frac{Ixxs}{A_S}(\frac{9}{5}\beta^5-12\beta^3+36\beta)
\end{bmatrix}$$

(4.22)

where,

$$BG1 = \frac{1}{2}(-\sin\beta\cos\beta + \beta)$$

$$BG2 = \sin\beta - \beta\cos\beta$$

$$BG3 = -4\cos\beta + \beta^2\cos\beta - 2\sin\beta + 4$$

$$BG5 = -\cos\beta - \sin\beta + 1$$

$$BG5 = -4\sin\beta + \beta^2\sin\beta - 2\beta\sin\beta$$

$$B1 = \frac{1}{2}(\cos^2\beta - 1)$$

$$B2 = \cos\beta + 1$$

4.2.3 Mass matrix of out-of-plane vibration of a curved beam

If equation 4.18 is substituted into the strain energy equations 4.14, 4.15 and 4.16, the mass matrix is obtained as,

$$
[m]_o = \rho_s A_s R^2
\begin{bmatrix}
(AACSQ) & (CSQAA) & C & -C1 & (CAA-\frac{C2}{2}) & -CA & (-C1AA) & AA(2C-C2) & AA(6C1-C3) \\
 & (SSQAA) & S & -S1 & (SAA-\frac{S2}{2}) & -SA & (-S1AA) & AA(2S-S2) & AA(6S1-S3) \\
 & & \beta & \frac{\beta^2}{2} & (\beta-\frac{\beta^3}{6}) & 0 & \frac{\beta^2}{2} & (2\beta-\frac{\beta^3}{3}) & (3\beta^2-\frac{\beta^4}{4}) \\
 & & & \frac{\beta^3}{3} & (-\frac{\beta^2}{2}+\frac{\beta^4}{8}) & 0 & \frac{\beta^3}{3} & (-\beta^2+\frac{\beta^4}{4}) & (3\beta^2-\frac{\beta^4}{4}) \\
 & & & & (AA\beta-\frac{\beta^3}{3}+\frac{\beta^5}{20}) & -A\beta & (\beta^2\frac{AA}{2}+\frac{\beta^4}{8}) & ((2\beta-\frac{\beta^3}{3})AA-\frac{\beta^3}{3}+\frac{\beta^5}{10}) & ((3\beta^2-\frac{\beta^4}{4})AA-\frac{3\beta^4}{4}+\frac{\beta^6}{12}) \\
 & & & & & A\beta & (A\frac{\beta^2}{2}) & (A(2\beta+\frac{\beta^3}{3})) & (A(-3\beta^2+\frac{\beta^4}{4})) \\
 & & & & & & AA\frac{\beta^3}{3} & AA(\beta^2+\frac{\beta^4}{4}) & AA(2\beta^3+\frac{\beta^5}{5}) \\
 & & & & & & & AA(4\beta-4\frac{\beta^3}{3}+\frac{\beta^5}{5}) & AA(6\beta^2-2\beta^4+\frac{\beta^6}{6}) \\
 & & & & & & & & AA(12\beta^3-\frac{12}{5}\beta^5+\frac{\beta^7}{7})
\end{bmatrix}
$$

(4.23)

where,

$$CSQ = (\beta + \frac{\sin(2\beta)}{2}) / 2$$

$$SSQ = (\beta - \frac{\sin(2\beta)}{2}) / 2$$

$$C = \sin(\beta)$$

$$S = -\cos(\beta) + 1$$

$$C1 = \cos(\beta) - 1 + \beta \sin(\beta)$$

$$C2 = 2\beta \cos(\beta) + (\beta^2 - 2)\sin(\beta)$$

$$C3 = 3\beta^2 \cos(\beta) + 6(\cos(\beta) - 6(\cos(\beta) - 1) + (\beta^3 - 6\beta)\sin(\beta)$$

$$S1 = \sin(\beta) + \beta \cos(\beta)$$

$$S2 = 2\beta \sin(\beta) + 2(\cos(\beta) - 1) - \beta^2 \cos\beta$$

$$S3 = (3\beta^2 - 6)\sin(\beta) + (6\beta - \beta^3)\cos(\beta)$$

$$A = \frac{I_P}{A_S R^2}$$

$$AA = 1 + A$$

CHAPTER FIVE
DISCUSSIONS OF RESULTS

In this chapter, some of the results obtained for the frequencies and buckling loads of curved beams in out-of-plane directions is shown and compared with some other researchers' results in order to indicate the degree of accuracy and adaptability that can be expected in the application of the finite element method. Moreover, the effects of opening angle, variations of cross-section, static and dynamic load parameters on the stability regions are shown in graphics.

The model shown in Figure 5.1 is used for the Finite Element analysis of the curved beam. In this study, C1, C2, C3, C4 and C5, represent different type cross-section curved beams. The explanation of these cross-sections is as follows:

C1: Uniform ($t_R = t_t$, $b_R = b_t$ Fig. 5.1a),
C2: Unsymmetric tapered with constant width (tR ≠tt, bR = bt Fig 5.1b.),
C3: Double unsymmetric tapered ($t_R \neq t_t$, $b_R \neq b_t$ Fig 5.1c.),
C4: Symmetric tapered with constant width ($t_R \neq t_t$, $b_R = b_t$ Fig 5.1d.),
C5: Double symmetric tapered ($t_R \neq t_t$, $b_R \neq b_t$ Fig 5.1e.).

The first four natural frequencies obtained with the present element were compared with the analytical results of Ojalvo and Newman (1964) and given in Table 5.1. In addition, the critical buckling load for various opening angles the uniform cross-section beam were compared with the results of Timoshenko (1961) and given in Table 5.2.

As seen from the Tables (5.1 and 5.2,) agreement between the results obtained by in both tables is very good.

In Table 5.3 the natural frequencies of curved beams with fixed- fixed end conditions and three different opening angles are compared with Sabuncu' s(1978) and Rao's (1970) results. As shown from the table 5.3 torsional frequencies (T1 and T2) are obtained, when the internal node is used.

In table 5.4 and 5.5 for different opening angels the frequencies and critical buckling loading of curved beams with different opening angles and cross-sections are given for the first five modes. It can be seen that the results with and without internal nodes are similar.

In table 5.6 and table 5.7 the dynamic unstable regions of curved beams which have different cross-section without and with internal nodes are given inceptively. It can be seen that the result obtained from two different finite element models are good.

Figure 5.2 shows that the effect of variation of opening angle of an arch on the fundamental frequency parameter for various cross-sections. It can be noticed from the figure that when the opening angle of an arch increases, the fundamental frequency parameter decreases for all the cross-sections as expected. It can also be noticed that the frequency parameters of C1, C2, C5 cross-sectioned curved beams are fairly close. Between 30^0 and 60^0 opening angles, the fundamental frequencies of C3 and C4 cross-sectioned curved beams are more apart than the fundamental frequencies of other type cross-sectioned curved beams.

When the opening angle of an arch increases, the fundamental frequency parameters of curved beams having the same length but five different cross-sections come closer. This phenomenon can be explained as follows: when the opening angle of an arch increases, the length of curved beams also increases, consequently beams become very flexible. The length variation effect on the flexibility is more dominant than the effect of variation of cross-section.

As shown in Figure 5.3, if the variation of the cross-section diminishes and approaches the uniform cross-section, the fundamental frequencies of C2 and C5 cross-sectioned curved beams increase and approach the frequency parameter of C1 cross-sectioned curved beam. On the other hand, the fundamental frequencies of C3 and C4 cross-sectioned curved beams decrease and approach the fundamental frequency of the C1 cross-sectioned curved beam.

Effect of opening angle of curvature on the critical buckling load is shown in Figure 5.4. When the opening angle of an arch increases, as a result the curved beam becomes more flexible. Thus, as shown in the figure, the critical buckling load decreases. It can be noticed from the figure that critical buckling load values of beams having C2 and C4 type cross-sections are close to each other. There is a similar phenomenon between C3 and C5 type cross-sectioned curved beams. Critical buckling loads of single tapered curved beams (C2 and C4) are higher than the double tapered curved beams (C3 and C5), respectively, as expected. It can also be noticed that even though the thickness of C4 tapers twice as much as C2 and the thickness and width of C5 tapers twice as much as C3 type beams. It seems that symmetric tapered beams are more stable than expected.

Figure 5.5 shows that the effects of thickness variation of a curved beam on the critical buckling load for various cross-sections. It is seen that when the variation of cross-section diminishes and approaches the uniform cross-section, the curved beam becomes stiffer; as a result, the critical buckling load increases and takes the value of the uniform cross-sectioned curved beam. From this figure, it can be said that static stability values of curved beams having C3, C5, C2 and C4 type cross-sections increase, respectively. This increase decreases as the cross-section variation diminishes.

From figure 5.6, it can be noticed that the first dynamic instability region widens because of the increase in the opening angle of the arch. C4 cross-sectioned curved beam is less stable compared to other cross-sections. In addition, when the dynamic load parameter increases, the unstable region widens.

As shown in figure 5.7, when the compared with figure 5.6, if the static load parameter increases, the increases, the initial ratio of the disturbing frequency to the fundamental frequency moves towards origin. It can be seen from the figures that the curved beam under periodic loading becomes unstable at a small disturbing frequency and small dynamic load parameter.

Figure. 5.8 and figure 5.9 show that when b_t/b_r and t_t/t_r ratios approach unity for $\alpha=0$ and $\alpha=0.2$, the first unstable region approaches the region C1 cross-sectioned curved beam. In both figures, the order of the unstable regions of all cross-sections does not change from the stability point of view.

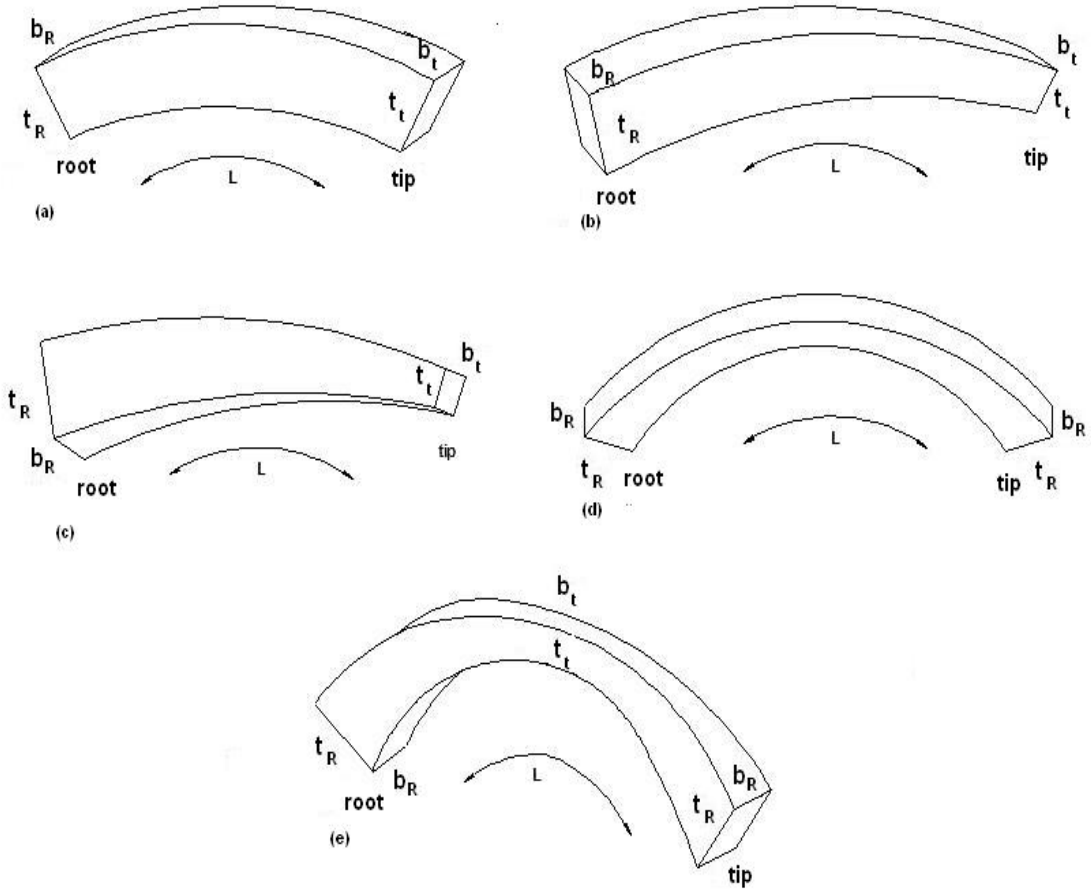

Figure 5.1Cross-sections of curved beams (a) uniform (C1, $t_R = t_t$, $b_R = b_t$); unsymmetric tapered with constant width (C2, $t_R \neq t_t$, $b_R = b_t$); (c) double unsymmetric tapered (C3, $t_R \neq t_t$, $b_R \neq b_t$.);(d) symmetric tapered with constant width(C4, $t_R \neq t_t$, $b_R = b_t$); (e) double symmetric tapered (C5, $t_R \neq$tt, $b_R \neq b_t$).

Table 5.1 Comparison of out-of plane frequencies of a cantilever curved beam obtained by using the present finite element method and the results of other study, t=0.0127 m, b=0.0127 m, R=0.0254 m, ρ=2770 kg/m3, E=6.89e10 N/m2, β=270^o

Mode	Natural Frequency (Hz)		
	FEM without Internal Node (12 element)	**FEM with Internal Node (3 element)**	**Ojalvo & Newman (1961)**
1	9.7	10.00	8.48
2	23.19	23.40	22.26
3	70.48	71.8	72.56
4	176.46	178.50	171.5

Table 5.2 Comparison of the critical buckling load obtained for various opening angles of a fixed-fixed boundary conditioned beam. (t=0.001587 m, b=0.02753 m, R=0.3556 m)

Opening Angle	Critical Buckling Load(P_{cr})(kN/m)		
	FEM without Internal Node (12 element)	**FEM with Internal Node (3 element)**	**Timoshenko (1964)**
30	1815.79	1802.00	1814.8
45	777.73	774.80	775.40
60	418.70	417.20	413.01
90	167.71	166.80	164.1

Table 5.3 Comparison of out-of plane frequencies ratio of a fixed-fixed curved beam obtained by using the present finite element method and the results of other studies**,** t=0.0127 m, b=0.0127 m, R=0.0254 m, ρ=2770 kg/m^3, E=6.89e10 N/m^2, β=270^o

		$\lambda = p\sqrt{\rho A_s R^4 / E_s I_{yys}}$		
Subtended Angle	**Mode**	**Rao Classical Theory (1970)**	**M.Sabuncu (1978)**	**Present With Internal Node**
180^0	1	1.839	1.800	1.800
	2	5.305	5.047	5.048
	T1	-	7.073	7.077
	3	11.108	10.165	10.169
	T2	-	11646	11.656
	4	19.006		17.132
270^0	1	0.758	0.754	0.755
	2	2.000	1.969	1.970
	3	4.406	4.243	4.235
	T1	-	5.956	5.939
	4	7.822	7.446	7.448
360^0	1	0.438	0.435	0.435
	2	0.952	0.957	0.957
	3	2.137	2.119	2.119
	4	3.965	3.916	3.916

Table 5.4 Comparison of out-of plane frequencies of a fixed-fixed curved beam obtained by using the with and without internal nodes the finite elements, t=0.04 m, b=0.002m, R=0.254 m, ρ=2770 kg/m^3, E=6.89e10 N/m^2.

Subtended Angle (Degrees)	Mode	Natural Frequency (Hz)									
		C1		C2		C3		C4		C5	
		FEM Without Internal Node	FEM With Internal Node	FEM Without Internal Node	FEM With Internal Node	FEM Without Internal Node	FEM With Internal Node	FEM Without Internal Node	FEM With Internal Node	FEM Without Internal Node	FEM With Internal Node
90	1	120.30	121.00	120.00	121.00	90.30	91.00	138.00	133.51	121.60	119.56
	2	344.00	344.00	342.10	343.00	252.40	246.40	358.50	350.27	344.80	261.22
	3	683.80	684.00	681.70	685.00	500.10	513.60	698.40	683.52	685.00	494.69
	4	1137.60	1140.00	1135.50	1140.00	830.90	831.30	1150.40	1138.71	1142.20	857.51
	5	1705.40	1732.00	1703.30	1703.00	1244.70	1245.60	1719.20	1710.23	1283.20	1283.78
120	1	65.50	65.40	64.70	65.10	49.20	49.70	75.50	72,80	72.80	66.65
	2	188.80	188.80	187.60	188.00	138.70	135.50	197.10	192.56	160.90	144.88
	3	379.40	379.40	378.00	379.90	277.50	285.00	387.50	378.55	300.60	274.89
	4	634.40	636.00	633.00	635.80	463.30	463.60	641.40	634.75	485.50	478.31
	5	953.60	968.40	952.20	967.00	696.00	696.90	961.20	955.53	718.00	718.01
150	1	40.10	40.10	39.70	39.90	30.60	30.90	47.00	45.17	46.60	42.37
	2	117.10	117.10	116.20	116.60	86.20	84.30	122.50	119.70	101.20	91.13
	3	238.50	238.60	237.50	238.80	174.50	179.20	243.70	237.92	189.80	173.20
	4	401.50	402.60	406.50	402.30	293.20	293.50	405.80	401.50	307.80	302.82
	5	605.60	615.10	849.70	841.20	442.00	442.70	610.30	606.79	456.40	456.09

Subtended Angle (Degrees)	Mode	C1		C2		C3		C4		C5	
		FEM Without Internal Node	FEM With Internal Node	FEM Without Internal Node	FEM With Internal Node	FEM Without Internal Node	FEM With Internal Node	FEM Without Internal Node	FEM With Internal Node	FEM Without Internal Node	FEM With Internal Node
180	1	26.90	26.90	26.60	26.70	20.80	21.10	32.00	30.66	32.60	29.40
	2	78.30	78.30	77.60	77.90	57.70	56.50	82.20	80.27	68.90	62.04
	3	162.10	162.10	161.20	162.20	118.60	121.80	165.60	161.58	129.80	118.00
	4	275.00	275.80	274.10	275.50	200.90	201.10	277.90	274.83	211.40	207.50
	5	416.60	423.30	415.70	422.50	304.00	304.60	419.70	417.35	314.30	313.81
270	1	12.73	12.70	12.39	12.50	10.20	10.30	15.16	14.50	15.74	13.99
	2	29.98	30.00	26.63	29.90	22.43	22.10	32.12	31.33	28.70	25.90
	3	65.78	65.90	65.27	65.80	48.29	49.60	67.39	65.54	54.14	48.57
	4	115.35	115.80	114.76	115.60	84.32	84.50	116.51	115.05	89.56	87.28
	5	177.97	181.00	177.33	180.60	129.92	130.20	179.18	178.20	134.97	134.26

Table5.5 Comparison of out-of plane static stability (buckling loading) of a fixed-fixed curved beam obtained by using the finite elements with and without internal nodes results, t=0.04 m, b=0.002m, R=0.254 m, ρ=2770 kg/m^3, E=6.89e10 N/m^2.

Subtended Angle (Degrees)	Mode	Critical Buckling Load(P_{cr})(N/m)									
		C1		C2		C3		C4		C5	
		FEM Without Internal Node	FEM With Internal Node	FEM Without Internal Node	FEM With Internal Node	FEM Without Internal Node	FEM With Internal Node	FEM Without Internal Node	FEM With Internal Node	FEM Without Internal Node	FEM With Internal Node
90	1	6330.00	6330.00	4585.00	4660.00	1635.00	1750.00	4758.00	4832.91	1945.00	2207.29
	2	13757.00	13770.00	10004.00	9900.00	3466.00	3320.00	10079.00	9662.72	3538.00	3320.20
	3	27771.00	27860.00	20199.00	20500.00	6949.00	7310.00	20203.00	20138.57	7179.00	6826.18
	4	42436.00	42920.00	30901.00	31700.00	10613.00	11410.00	30913.00	31708.53	10620.00	10685.73
	5	63626.00	67750.00	46329.00	48720.00	15913.00	18150.00	46360.00	47597.74	16174,00	17926.37
120	1	3266.00	3270.00	2362.00	2400.00	864.50	930.00	2520.00	2543.59	1089.50	1210.77
	2	7360.00	7370.00	5342.00	5300.00	1865.40	1780.00	5411.00	5187.57	1940.20	1818.86
	3	15240.00	15300.00	11047.00	11250.00	3815.00	4030.00	11077.00	11055.20	3975.20	3791.14
	4	23470.00	23750.00	17078.00	17530.00	5866.40	6300.00	17091.00	17523.70	5891.00	5931.10
	5	35392.00	37700.00	25758.00	27100.00	8844.60	10070.00	25784.00	26444.78	9008.10	9973.92
150	1	1904.00	1910.00	1377.00	1400.00	519.60	564.00	1516.00	1519.83	697.60	756.08
	2	4416.00	4430.00	3199.00	3180.00	1129.20	1075.00	3263.00	3128.34	1202.90	1126.59
	3	9455.00	9490.00	6826.00	6970.00	236.90	2515.00	6866.00	6861.69	2488.30	2390.43
	4	14698.00	14880.00	10685.00	10970.00	3672.40	3931.00	10698.00	10963.37	3704.00	3731.31
	5	22330.00	23800.00	16242.00	17100.00	5567.00	6338.00	16266.00	16660.97	5694.30	6294.43

Subtended Angle (Degrees)	Mode	C1		C2		C3		C4		C5	
		FEM Without Internal Node	FEM With Internal Node	FEM Without Internal Node	FEM With Internal Node	FEM Without Internal Node	FEM With Internal Node	FEM Without Internal Node	FEM With Internal Node	FEM Without Internal Node	FEM With Internal Node
180	1	1219.00	1220.00	881.00	897.00	344.00	376.00	1002.00	9979.21	488.90	515.43
	2	2835.00	2840.00	2049.00	2043.00	734.10	699.00	2109.00	2022.28	804.80	753.33
	3	6329.00	6360.00	4588.00	4667.00	1590.70	1697.00	4592.00	4595.31	1685.20	1634.23
	4	9938.00	10070.00	7217.00	7414.00	2483.40	2650.00	7231.00	7040.52	2157.90	2537.40
	5	15242.00	16250.00	11078.00	116580.00	3803.80	4311.00	11101.00	11353.42	3897.20	4297.24
270	1	571.40	572.00	400.00	407.00	165.00	181.00	475.30	468.76	241.60	234..34
	2	923.80	928.00	665.70	670.00	262.30	254.00	715.50	685.49	314.20	296.04
	3	2475.10	2491.00	1784.20	1820.00	637.80	691.00	1790.30	1798.19	695.50	708.87
	4	3960.80	4021.00	2865.70	2952.00	995.70	1049.00	2879.40	2940.02	1029.60	1035.70
	5	6329.40	6765.00	4586.90	4852.00	1581.80	1767.00	4610.90	4685.63	1643.50	1784.24

Table 5.6 The effect of dynamic load parameter on the first dynamic stability region of curved beams for various cross-sections The Finite Element Model has no internal node, $b_R/b_t = t_R/t_t$=1(C1), b_R/b_t = 1 and t_R/t_t=0.5 (C2 and C4),$b_R/b_t = t_R/t_t$=0.5 (C3 and C5), α=0, β= 120^0, t=0.04 m, b=0.002m, R=0.254 m, ρ=2770 kg/m^3, E=6.89e10 N/m^2.

β_d	**Dynamic First Unstable Region Without Internal Node (Hz)**									
	C1		C2		C3		C4		C5	
	uniform		non-uniform wcw		double non-uniform		centrally symmetric		centrally symmetric	
0	130,943	130,943	129,469	129,469	98,433	98,433	150,904	150,904	145,513	145,513
0,5	113,796	145,935	112,572	144,226	86,049	109,146	131,46	167,812	128,022	160,436
1	93,269	159,387	92,32	157,465	71,022	118,686	108,039	182,927	106,431	173,579
1,5	66,228	171,686	65,601	169,559	50,859	127,35	76,95	196,693	76,841	185,4
2	0	183,073	0	180,751	0	135,328	0	209,398	0	196,219

Table 5.7 The effect of dynamic load parameter on the first dynamic stability region of curved beams for various cross-sections have used to The Finite Element Model has internal node, $b_R/b_t = t_R/t_t$=1(C1), b_R/b_t = 1 and t_R/t_t=0.5 (C2 and C4), $b_R/b_t = t_R/t_t$=0.5 (C3 and C5), α=0 β= 120^0 t=0.04 m, b=0.002m, R=0.254 m, ρ=2770 kg/m^3, E=6.89e10 N/m^2.

β_d	**Dynamic First Unstable Region With Internal Node (Hz)**									
	C1		C2		C3		C4		C5	
	uniform		non-uniform		double non-uniform		centrally symmetric		centrally symmetric	
0	130,841	130,841	129,461	129,461	98,586	98,586	150,805	150,805	145,498	145,498
0,5	113,707	145,817	112,565	144,215	86,185	109,313	131,27	167,795	127,96	160,322
1	93,196	159,263	92,315	157,453	71,135	118,865	108,32	182,916	106,354	173,47
1,5	66,176	171,552	65,598	169,545	50,941	127,539	76,203	196,58	76,56	185,323
2	0	182,93	0	180,735	0	135,526	0	209,29	0	196,192

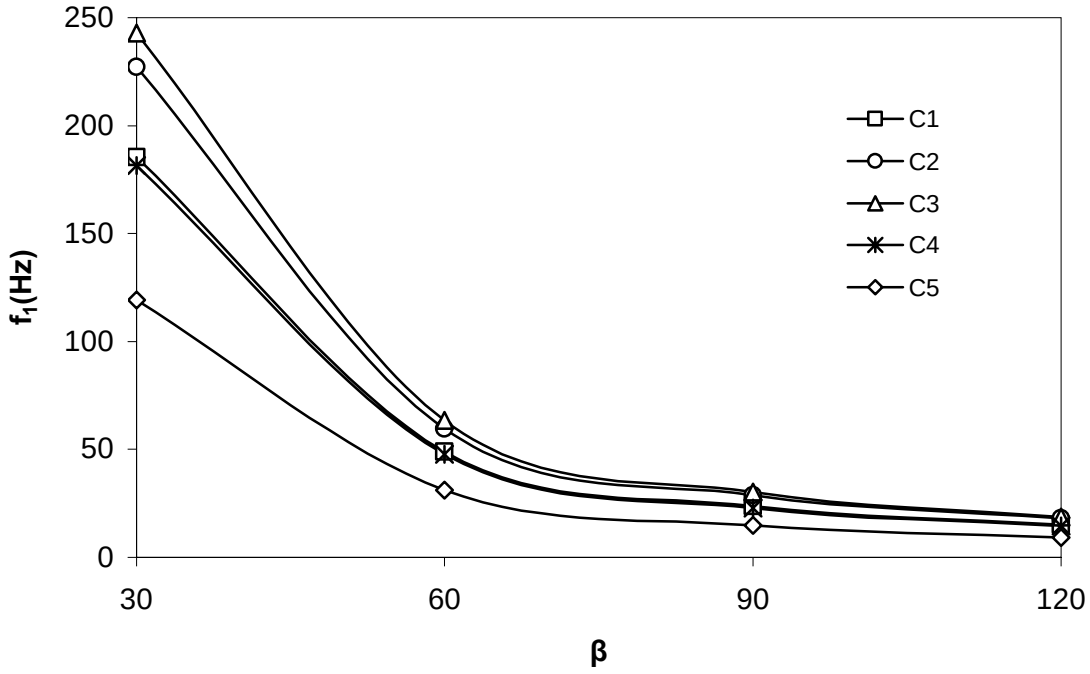

Figure.5.2 The effect of variation of opening angle of an arch on the fundamental frequency for various cross-sections, $b_R/b_t = t_R/t_t=1$(□ C1), $b_R/b_t = 1$ and $t_R/t_t=0.5$ (O C2 and * C4), $b_R/b_t = t_R/t_t=0.5$ (Δ C3 and◊ C5).

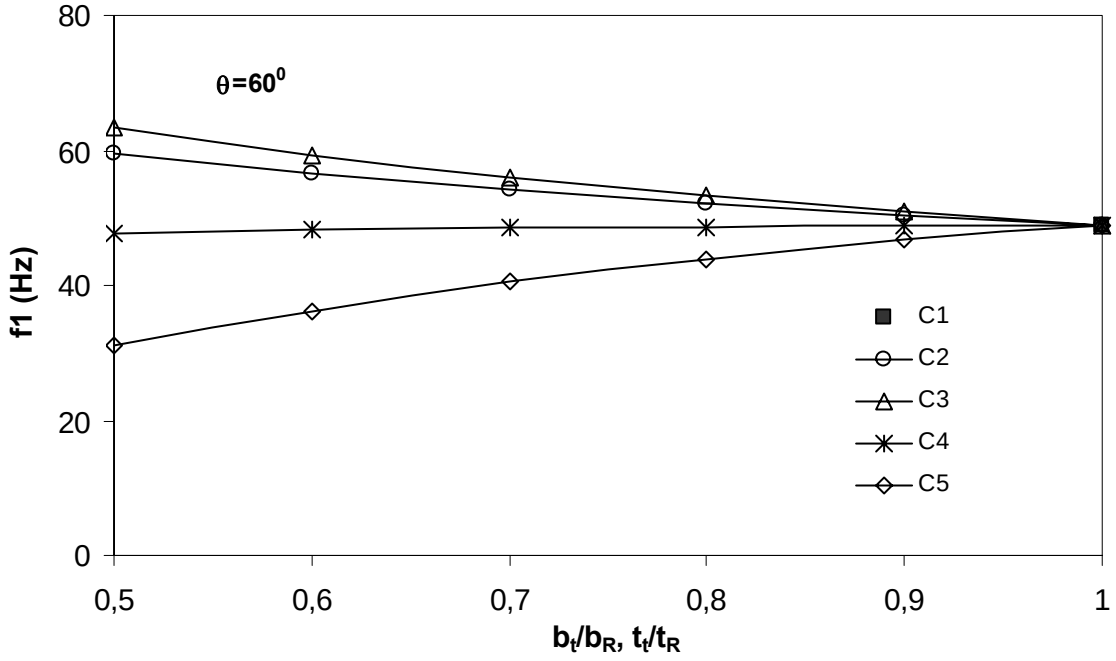

Figure 5.3 The variation of the free vibration frequency with various ratio of cross-section. $\beta = 60^0$,$b_R=b_t$, $t_R=t_t$ (■ C1), $b_R=b_t$ and $t_R\neq t_t$ (O C2 and * C4), $b_R/b_t = t_R/t_t=0.5$ (Δ C3 and ◊ C5),

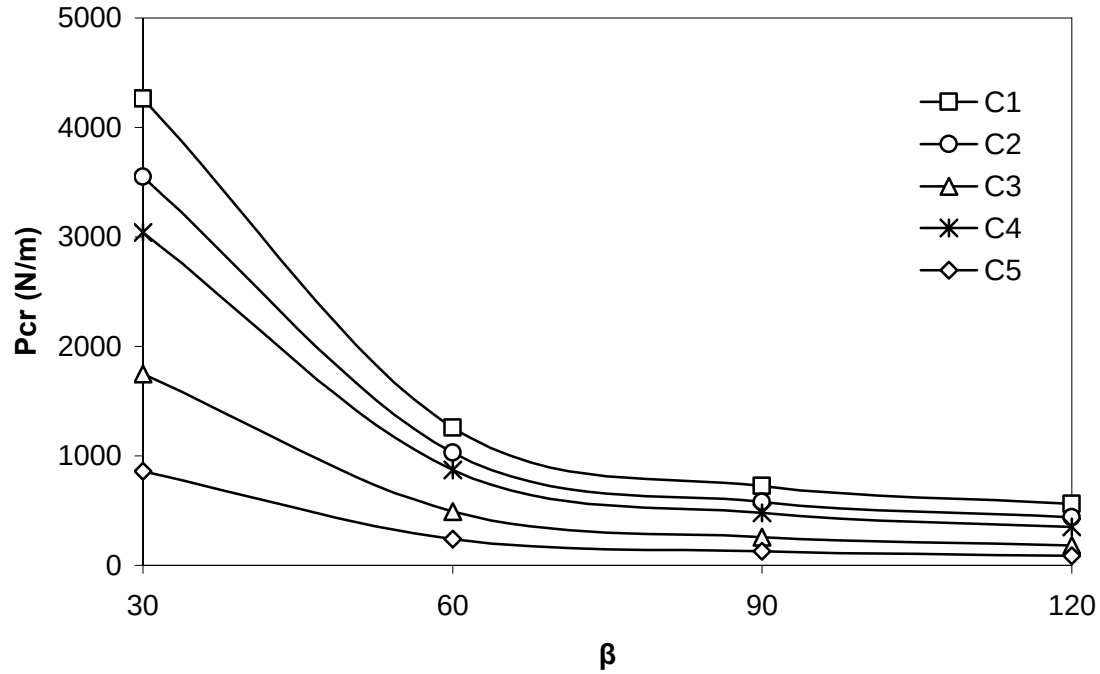

Figure. 5.4 The variation of the critical buckling load with various cross-section and curve radius, $b_R/b_t = t_R/t_t=1$(□ C1), $b_R/b_t = 1$ and $t_R/t_t=0.5$ (O C2 and * C4), $b_R/b_t = t_R/t_t=0.5$ (Δ C3 and◊ C5).

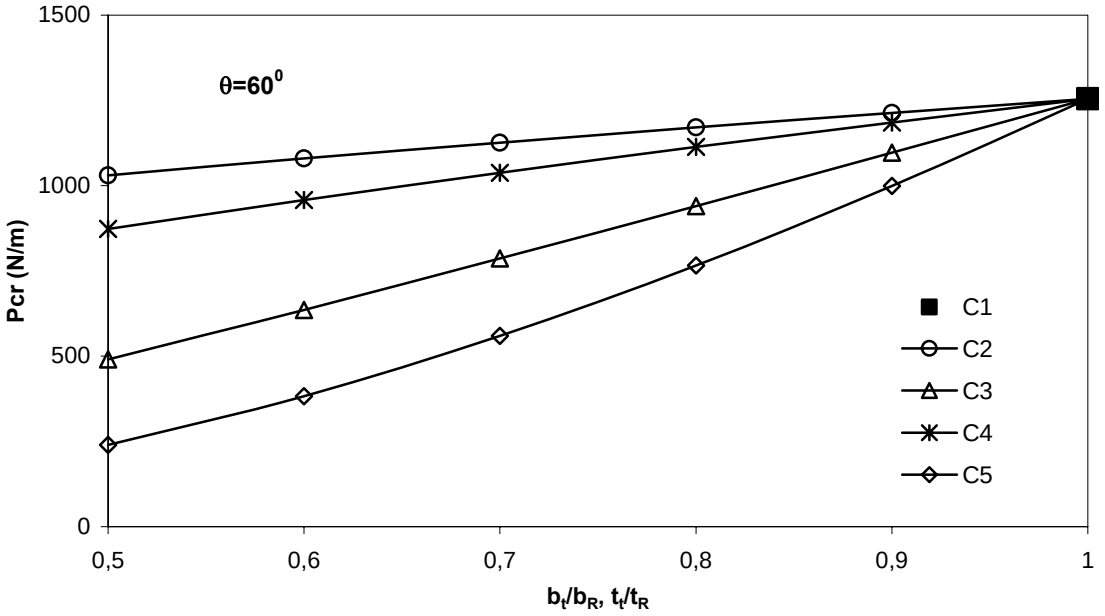

Figure 5.5 The variation of the critical buckling load with various ratio of cross-section, $\beta = 60^0$, $b_R=b_t$, $t_R=t_t$ (■ C1), $b_R=b_t$ and $t_R \neq t_t$ (O C2 and * C4), $b_R/b_t = t_R/t_t=0.5$ (Δ C3 and ◊ C5),

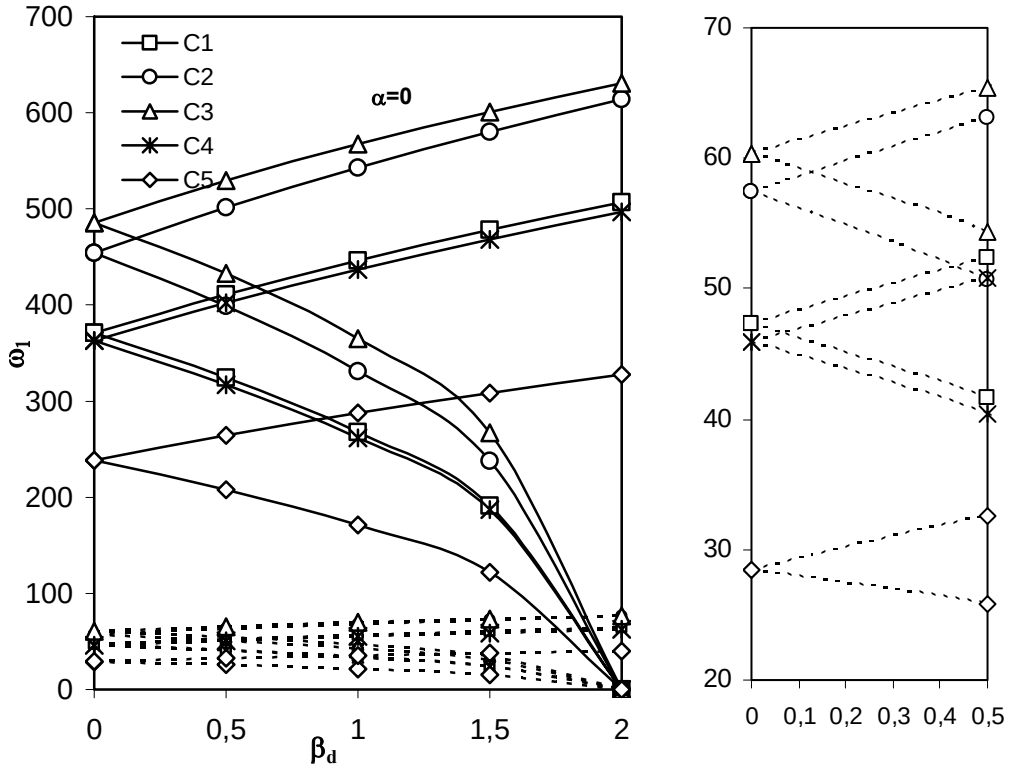

Figure 5.6 The effect of dynamic load parameter on the first dynamic stability region of curved beams for various cross-sections and two different opening angels. . $\alpha = 0$. $b_R/b_t = t_R/t_t = 1$(C1), $b_R/b_t = 1$ and $t_R/t_t = 0.5$ (O C2 and * C4), $b_R/b_t = t_R/t_t = 0.5$ (Δ C3 and ◊ C5), …… $\beta = 90^0$, _____ $\beta = 30^0$

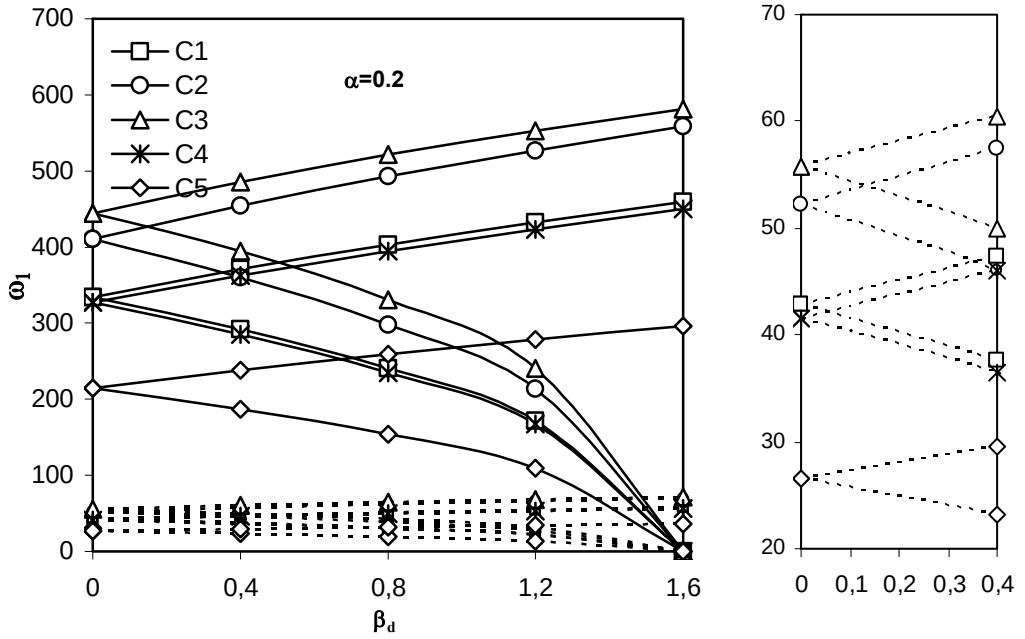

Figure 5.7 The effect of dynamic load parameter on the first dynamic stability region of curved beams for various cross-sections and two different opening angels. $\alpha = 0.2$. $b_R/b_t = t_R/t_t = 1$ (□ C1), $b_R/b_t = 1$ and $t_R/t_t = 0.5$ (O C2 and * C4), $b_R/b_t = t_R/t_t = 0.5$ (Δ C3 and ◊ C5), … $\beta = 90^0$, _____ $\beta = 30^0$

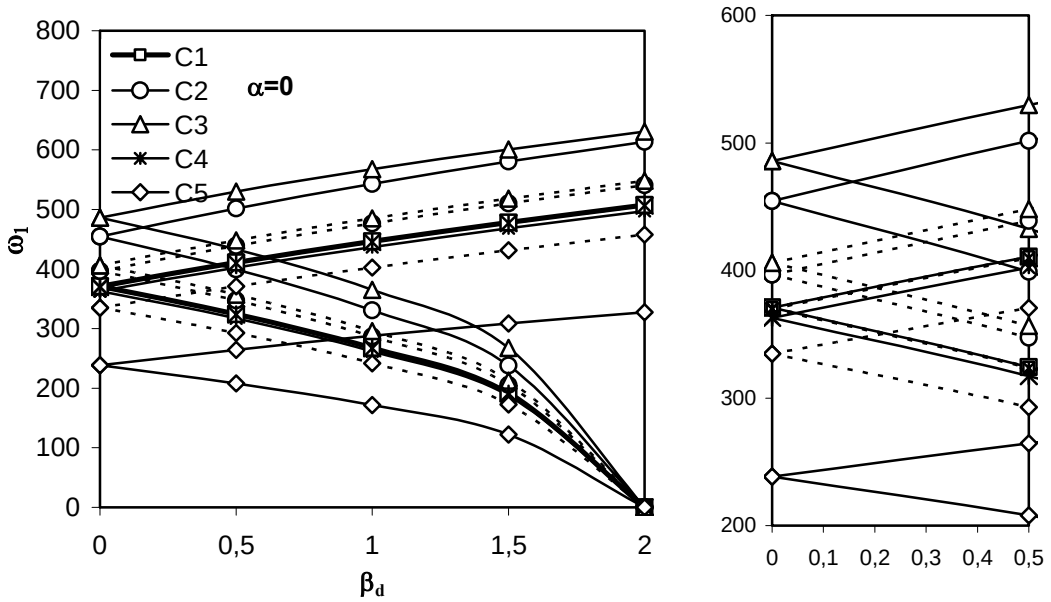

Figure 5.8 The effect of dynamic load parameter on the first dynamic stability region of curved beams for various cross-sections and two different opening angels. $\alpha = 0$, $\beta = 30^0$, $b_R = b_t$, $t_R = t_t$ ------ $b_R/b_t = t_R/t_t = 1$(□ C1), ____$b_R/b_t = 1$ and $t_R/t_t = 0.5$ (O C2 and * C4), $b_R/b_t = t_R/t_t = 0.5$ (Δ C3 and ◊ C5) , ……. $b_R/b_t = t_R/t_t = 1$(□ C1), $b_R/b_t = 1$ and $t_R/t_t = 0.8$ (O C2 and * C4), $b_R/b_t = t_R/t_t = 0.8$ (Δ C3 and ◊ C5))

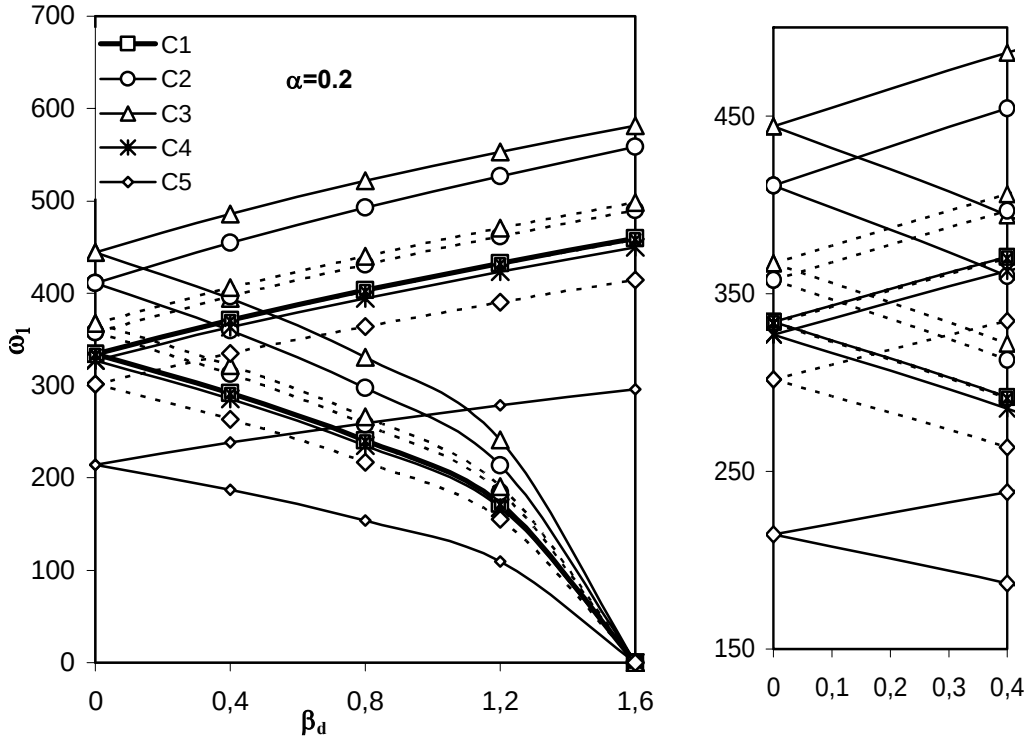

Figure 5.9 The effect of dynamic load parameter on the first dynamic stability region of curved beams for various cross-sections and two different opening angels. α= 0.2, β= 30^0 , b_R=b_t, t_R=t_t ---- $b_R/b_t = t_R/t_t$=1(□ C1), ____b_R/b_t = 1 and t_R/t_t=0.5 (O C2 and * C4), $b_R/b_t = t_R/t_t$=0.5 (Δ C3 and ◊ C5) , ……. $b_R/b_t = t_R/t_t$=1(□ C1), b_R/b_t = 1 and t_R/t_t=0.8 (O C2 and * C4), $b_R/b_t = t_R/t_t$=0.8 (Δ C3 and ◊ C5))

CHAPTER SIX
CONCLUSIONS

In this thesis out of plane free vibration, static and dynamic stability analysis of curved beam for various cross-sections and opening angles are studied and the following conclusions are drawn.

The finite element method used in this investigation is ideal for the vibration, static and dynamic stability analysis of curved beam. The results show the finite element method give very good accuracy, when the compare with the results of other investigators.

The results obtained for vibration, static and dynamic stabilities, using the FEM with and without internal node are very close. In addition the finite element model with internal node has the advantage of using less number of elements in the analysis than without internal model.

When the subtended angle increases, the static stability (buckling load) and the firs fundamental frequency of curved beam decreases, this phenomenon can also be explained as follows; when the subtended angle of a curved beam increases, the length of curved beams also increases, consequently beam becomes very flexible.

The effect of variation of t_t/t_r and b_t/b_r ratio on the static stability (buckling load) of a curved beam, when the t_t/t_r and b_t/b_r ratio increases the static stability (buckling load) of a curved beam also increases. If the variation of the cross-section diminishes and approaches the uniform cross-section, the fundamental frequencies of C2 and C5 cross-sectioned curved beams increase and approach the frequency parameter of C1 cross-sectioned curved beam. On the other hand, the fundamental frequencies of C3 and C4 cross-sectioned curved beams decrease and approach the fundamental frequency of the C1 cross-sectioned curved beam.

When the subtended angle of a curved beam increases, the first dynamic instability regions widen.

If the static load parameter increases, the initial ratio of natural frequency to the fundamental frequency moves towards origin.

When the t_t/t_r and b_t/b_r ratios approach unity, the unstable region approaches the region of C1 cross-sectioned curved beam as expected in figure 5.8 and figure 5.9

If the static load parameter is equal to 0.2, in the initial disturbing frequency moves towards origin. The dynamic load parameter is bounded between the values of zero and 1.6.

Finally, by changing the static and dynamic load parameters, type of the cross-section of a curved beam, (the ratios of dimensions of thickness and width at the tip cross-section to the ones at the root cross-section of the curved beam), dynamic stability of curved beam may be conserved.

REFERENCES

Belek, H. T. (1977). *Vibration characteristics of shrouded blades on rigid and flexible disks*. Ph. D. Thesis, University of Surrey, U.K.

Briseghella, L., Majorana, C. E. and Pelegrino, C. (1998). Dynamic stability of elastic structures: a finite element approach, *Computers & Structures*, *69*, 11-25.

Bolotin, V. (1964), *The dynamic stability of elastic systems*. Holden-Day, San Francisco.

K.J. Kang, C.W. Bert and A.G. Striz (1995), "Vibration and Buckling Analysis of Circular Arches Using DQM" *Computers & Structures*,60(1), 49-57.

Liu, G. R. and Wu, T. Y. (2001). In-plane vibration analyses of circular arches by the generalized differential quadrature rule. *International Journal of Mechanical Sciences*, 43, 2597-2611.

M.Kawakami, T. Sakiyama, H.Matsuda, C. Morita, (1995), "In Plane and Out- of- Plane Free Vibrations of Curved Beams with Variable Cross sections", *Journal of Sound and Vibration*, 187(3), 381-401.

M. R. Banan , G. Karami and Farshad (1990), "Finite Element Stability Analysis of Curved Beams on Elastic Foundation" *Mathematical and Computer Modeling*, 14, 1990, 863-867.

M.T. Piovan, V.H. Cortinez and R.E. Rossi, (2000), Out-of-plane vibrations of shear deformable continuous horizontally curved thin-walled beams, *Journal of Sound and Vibration* 237, (2000), 101–118.

Ojalvo, I. U. and Newman, M. (1964). Natural frequencies of clamped ring segments. *Machine design*, May, 21, 219-220.

Öztürk,H, Yeşilyurt, İ, and Sabuncu, M. (2006), "In Plane Analysis of Non-Uniform Cross-Sectioned Curved Beams", *Journal of Sound and Vibration*, 296, 277-291.

Papangelis, J. P. and Trahair, N. S. (1987). Flexural-torsional buckling of arches. *Journal of Structural Engineering*, *113* (4), 889-906.

Petyt M. and Fleischer C.C.(1971), "Free Vibration of Curved Beam", *Journal of Sound and Vibration*, 18(1), 17-30.

Sabir, A.B. and Ashwell, D.G.(1971), "A Comparasion of Curved Beam Finite Elements when Used in Vibration Problem" *Journal of Sound and Vibration*, 18, 555-563.

Sabuncu, M. (1978), *Vibration Caharacteristics of Rotating Aerofoil Cross-Section Bladed-Disc Assmbly*, Ph D. Thesis, University of Surrey.

S. Nair, V.K. Garg and Y.S. Lai (1985), "Dynamic Stability of A Curved rail Under A Moving Load" *Applied Mathematical Modeling*, 9, 220-224.

S. P. Timoshenko , J. M. Gere,(1991), *Theory of Elastic System* McGraw- Hill Book Company, New York, 1991.

S.Y. Lee and J.C. Chao (2000), "Out-of-Plane Vibrations of Curved Non-Uniform Beams of Constant Radius" *Journal of Sound and Vibration*, 238(3), 443-458.

Şakar, G., Öztürk, H. and Sabuncu, M. (2001). Stability analysis of curved beams. The Tenth National Machine Theory Symposium, Selcuk University, Konya, Turkey.

Timoshenko, S. P., & Gere, J. M. (1961). Theory of elastic stability (2nd ed.) McGraw-Hill; Newyork

Wu, J. S. and Chiang, L. K. (2003). Free vibration analysis of arches using curved beam elements. *International Journal for Numerical Methods in engineering*, 58, 1907-1936.

Yıldırım, V.(1996), "A computer program for the free vibration analysis of elastic arcs", *Computers & Structures*,62(3), 475-485.

Yoo, C.H., Kang Y. J. and Davidson, J. S.(1996), "Buckling Analysis of Curved Beams by Finite Element Discretization" *Journal of Engineering Mechanics*, 122(8), 762-770.

Yoo, C. H., and Pfeiffer, P. A.(1983). Elastic stability of curved members. *Journal of Structural Engineering*, *109* (12), 2922-2940.

Z.P. Bazant, L. Cedolin, (1991), *Stability of Structures*, Oxford University Press, New York.

LIST OF SYMBOLS

As	Area of curved beam cross section
Gs	Shear modulus of curved beam
Es	Modulus of elasticity of curved beam
f	Natural frequency
ρ	Density of curved beam
Ixxs	Second moment of area of cross section about axis X
Iyys	Second moment of area of cross section about axis Y
l	length of beam element
β	opening angle
βd	Dynamic component of load
α	Static component of load
R	Radius of curved beam
[M]	Global mass (inertia) matrix
[K]	Global stiffness matrix
[Kgo]	Global geometric stiffness matrix
b1	Width at the root of the curved beam
b2	Width at the top of the curved beam
t1	Thickness at the root of the curved beam
t2	Thickness at the top of the curved beam
$[\ ]^T$	Denotes transpose of a matrix
$[\ ]^{-1}$	Denotes inverse of a matrix
{ }	Denotes column matrix